Journal of Neurochemistry, 2007, **102**, 1658–1668 doi:10.1111/j.1471-4159.2007.04796.x

Reduced pain behaviors and extracellular signal-related protein kinase activation in primary sensory neurons by peripheral tissue injury in mice lacking platelet-activating factor receptor

Makoto Tsuda,* Satoshi Ishii,†‡ Takahiro Masuda,* Shigeo Hasegawa,* Koji Nakamura,* Kenichiro Nagata,* Tomohiro Yamashita,* Hidemasa Furue,§ Hidetoshi Tozaki-Saitoh,* Megumu Yoshimura,§ Schuichi Koizumi,¶ Takao Shimizu† and Kazuhide Inoue*

**Department of Molecular and System Pharmacology, Graduate School of Pharmaceutical Sciences, Kyushu University, Maidashi, Higashi-ku, Fukuoka, Japan*

†Department of Biochemistry and Molecular Biology, Faculty of Medicine, The University of Tokyo, Hongo, Bunkyo-ku, Tokyo, Japan

‡Precursory Research for Embryonic Science and Technology (PRESTO) of Japan Science and Technology Agency, Hongo, Bunkyo-ku, Tokyo, Japan

§Department of Integrative Physiology, Graduate School of Medical Sciences, Kyushu University, Maidashi, Higashi-ku, Fukuoka, Japan

¶Department of Pharmacology, Interdisciplinary Graduate School of Medicine and Engineering, University of Yamanashi, Shimokato, Chuo, Yamanashi, Japan

Abstract

Peripheral tissue injury causes the release of various mediators from damaged and inflammatory cells, which in turn activates and sensitizes primary sensory neurons and thereby produces persistent pain. The present study investigated the role of platelet-activating factor (PAF), a phospholipid mediator, in pain signaling using mice lacking PAF receptor (*pafr–/–* mice). Here we show that *pafr–/–* mice displayed almost normal responses to thermal and mechanical stimuli but exhibit attenuated persistent pain behaviors resulting from tissue injury by locally injecting formalin at the periphery as well as capsaicin pain and visceral inflammatory pain without any alteration in cytoarchitectural or neurochemical properties in dorsal root ganglion (DRG) neurons and a defect in motor function. However, *pafr–/–* mice showed no alterations in spinal pain behaviors caused by intrathecally administering agonists for *N*-methyl-D-aspartate (NMDA) and neurokinin$_1$ receptors. A PAFR agonist evoked an intracellular Ca^{2+} response predominantly in capsaicin-sensitive DRG neurons, an effect was not observed in *pafr–/–* mice. By contrast, the PAFR agonist did not affect C- or Aδ-evoked excitatory postsynaptic currents in substantia gelatinosa neurons in the dorsal horn. Interestingly, mice lacking PAFR showed reduced phosphorylation of extracellular signal-related protein kinase (ERK), an important kinase for the sensitization of primary sensory neurons, in their DRG neurons after formalin injection. Furthermore, U0126, a specific inhibitor of the ERK pathway suppressed the persistent pain by formalin. Thus, PAFR may play an important role in both persistent pain and the sensitization of primary sensory neurons after tissue injury.

Keywords: mitogen-activated protein kinase, platelet-activating factor receptor, primary afferent sensory neurons, tissue injury pain.

J. Neurochem. (2007) **102**, 1658–1668.

Received 5 January, 2007; revised manuscript received 27 April, 2007; accepted 30 May, 2007.

Address correspondence and reprint requests to Kazuhide Inoue, PhD, Department of Molecular and System Pharmacology, Graduate School of Pharmaceutical Sciences, Kyushu University, 3-1-1 Maidashi, Higashi-ku, Fukuoka 812-8582, Japan. E-mail: inoue@phar.kyushu-u.ac.jp

Abbreviations used: $[Ca^{2+}]_i$, intracellular Ca^{2+}; EPSC, excitatory postsynaptic current; CV, conduction velocity; ERK, extracellular signal-related protein kinase; fura-2AM, fura-2 acetoxymethylester; mcPAF, methylcarbamyl PAF; MEK, mitogen-activated protein kinase kinase; PAF, platelet-activating factor; PAFR, PAF receptor; septide, [pGlu^6, L-Pro^9]substance P (6–11); SG, substantia gelatinosa; TRPV1, transient receptor potential vanilloid type 1.

Primary afferent sensory neurons transmit sensory information received at the periphery to dorsal horn neurons in the spinal cord. Once peripheral tissue has been damaged, the damaged cells or surrounding inflammatory cells release a variety of mediators. Some stimulate directly nociceptors and elicit pain responses, and the others develop sensitization of primary sensory neurons to physical and chemical stimuli by activating intracellular protein kinases or by changing the gene expression and thereby result in enabling easier activation of the pain pathway. These events act together to create a persistent pain state (Julius and Basbaum 2001; Mayer *et al.* 2006).

Platelet-activating factor (PAF, 1-*O*-alkyl-2-acetyl-*sn*-glycero-3-phosphocholine) is a phospholipid mediator that regulates the functions of a variety of cells not only in the peripheral tissues but also in the nervous system (Ishii and Shimizu 2000; Prescott *et al.* 2000). The biological activities of PAF are elicited by activating its receptor, PAF receptor (PAFR), which belongs to the superfamily of G protein-coupled receptors (Honda *et al.* 1991; Ishii *et al.* 1998). Several studies have investigated the role of the PAF/PAFR system in modulating pain signaling. Local injection of PAF into the rat hindpaw increases the sensitivity to noxious stimulation (Bonnet *et al.* 1981; Belanger *et al.* 1987; Dallob *et al.* 1987). The lack of the response by injection of lyso-PAF (a structurally related, biologically inactive form) appears to involve PAFR (Belanger *et al.* 1987). Administering PAF into human skin also produces a hypersensitive state (Archer *et al.* 1984; Basran *et al.* 1984). These studies suggest that PAF might exaggerate pain. PAF is produced by various kinds of cells including keratinocytes (Alappatt *et al.* 2000) and inflammatory cells (Montrucchio *et al.* 2000), and the level of PAF is increased in inflamed tissue (Noguchi *et al.* 1989; Kihara *et al.* 2005; Doi *et al.* 2006). However, much less is known about the role of endogenous PAF/PAFR system in nociception. Although a recent behavioral study investigated this by means of pharmacological tools, such as BN52021, an antagonist for PAFR, the compound is not specific for PAFR since it was demonstrated to have antagonistic effects on glycine- and GABA-gated chloride channels (Kondratskaya *et al.* 2002; Ivic *et al.* 2003; Huang *et al.* 2004). In addition, some other PAFR antagonists have been reported to have an inverse agonistic effect (Dupre *et al.* 2001), an inhibitory effect on the activity of intracellular PAF acetylhydrolase, an inactivating enzyme of PAF (Adachi *et al.* 1997) or an antagonistic effect on histamine receptor (Merlos *et al.* 1997). Thus, these pharmacological problems of PAFR antagonists have been a major barrier to revealing the precise role of the endogenous PAF/PAFR system in pain signaling. Therefore, in the present study, we used mice that lack PAFR (*pafr*−/−) by targeted disruption of the gene (Ishii *et al.* 1998) and investigated the behavioral phenotype in a range of pain tests. Here we demonstrate that the PAF/PAFR system is important for persistent pain behaviors caused by tissue injury as well as capsaicin and visceral pain, and that the lack of PAFR results in a reduction of tissue injury-induced extracellular signal-related protein kinase (ERK) activation in primary afferent sensory neurons, an important kinase in sensitization (Dai *et al.* 2002; Obata and Noguchi 2004; Zhuang *et al.* 2004).

Materials and methods

Animals

All of the animals have been used in accordance with the guidelines of National Institute of Health Sciences, Kyushu University and The University of Tokyo. *pafr*−/− mice were established using a gene-targeting strategy (Ishii *et al.* 1998). Male *pafr*−/− mice and their wild-type littermates (9- to 11-week-old) used here have been backcrossed for 6–10 generations onto a C57BL/6 N genetic background. Within each experimental group, the sex ratio and the backcross generation were equal, and the age did not differ significantly. Male Wistar rats were also used some experiments.

Pain behavior studies

Noxious heat-evoked tail and hindpaw withdrawal responses were detected by the application of radiant heat (Ugo Basile, Italy) to the tail and the plantar surface of hindpaw, respectively (Tsuda *et al.* 1999a, 2000). The intensity of the heat stimulus was adjusted to 30 or 50 V, and the latency of the paw withdrawal response (s) was measured. The sensitivity to mechanical stimulus was assessed using von Frey filaments (0.02–2.0 g) (Stoelting, Wood Dale, IL, USA), and the mechanical stimulus producing the 50% paw withdrawal threshold was determined (Tsuda *et al.* 2003). In the tests of formalin- and capsaicin-induced pain, mice were injected intraplantarly with formalin (5%, 20 μL for mice; 2%, 100 μL for rats) and capsaicin (1.6 μg), respectively, and then the duration of the licking and biting responses to the injected hindpaw was recorded at 5 min intervals for 60 min after the injection (formalin pain) and for a period of 5 min (capsaicin pain) (Tsuda *et al.* 1999b). For the measurement of hindpaw swelling by formalin, the weights of the left (formalin) and right (phosphate-buffered saline) hind feet amputated at the ankle were measured 60 min after the injection of formalin. In the chemical visceral pain test, mice were injected i.p. with acetic acid (0.8%), and the number of abdominal writhes was counted for 5 min starting from 5 min after the injection. In the tests for pain responses at the spinal level, mice were injected intrathecally with NMDA (0.2 μg/5 μL) or with [pGlu^6, L-Pro^9]substance P (6–11) (septide; 10 μg/5 μL) (Sigma, St Louis, MO, USA), and the total duration of scratching, biting, and licking behaviors was recorded for 5 min (Sakurada *et al.* 1998). Motor coordination was assessed using the rotarod performance test (Tsuda *et al.* 1999b). For administering U0126, a mitogen-activated protein kinase kinase (MEK) inhibitor, under isoflurane anesthesia, a 32 gauge catheter (ReCathCo, Allison Park, PA, USA) was inserted through the atlanto-occipital membrane, and the tip of the catheter was positioned near the L5 dorsal root ganglion (L5 DRG). Rats were injected with U0126 (20 nmol/10 μL; Tocris, Bristol, UK) through the catheter 10 min before the injection of formalin into the hindpaw.

Intracellular calcium ($[Ca^{2+}]_i$) imaging

Acute dissociated DRGs from Wistar rats, wild-type and *pafr*−/− mice were used (Tsuda *et al.* 1999a, 2000). Cells were plated on poly-L-lysine-coated glass coverslips with silicon rubber walls (Flexiperm, W.C. GmbH, Germany). The increase in $[Ca^{2+}]_i$ in single cells was measured by the fura-2 technique (Koizumi *et al.* 1994). The cells were incubated with 5 μmol/L fura-2 acetoxymethylester (fura-2AM; Dojindo, Kumamoto, Japan) for 30 min in balanced salt solution (composition in mmol/L: NaCl 150, KCl 5, $CaCl_2$ 1.2, $MgCl_2$ 1.2, D-glucose 10 and HEPES 25; pH 7.4). Then, the cells were washed with balanced salt solution and mounted on an inverted fluorescence microscope (TMD-300, Nikon, Japan) equipped with a xenon-lamp and band-pass filters of 340 nm wavelength and 360 nm wavelength. The emission fluorescence was measured at 510 nm. Image data were processed by a Ca^{2+}-analysing system (Furusawa Lab. Appliance Co., Japan). KCl (75 mmol/L, 5 s), methylcarbamyl PAF (mcPAF: 1 μmol/L, 10 s) and capsaicin (1 μmol/L) were applied to the DRG neurons.

Patch-clamp recordings from substantial gelatinosa neurons of the spinal dorsal horn

We used spinal cord slice preparations from rats in order to precisely distinguish the effect of mcPAF between Aδ- and C-mediated excitatory post-synaptic currents (EPSCs) in SG neurons. A 600-μm thick transverse slice of the fifth lumber (L5) spinal cord with the L5 dorsal root from Wistar rat was cut using a vibratome (Yoshimura and Jessell 1989). The slice was placed on nylon mesh in the recording chamber, and then perfused at a rate of 10–15 mL min−1 with Krebs solution (composition in mmol/L: NaCl 117, KCl 3.6, $CaCl_2$ 2.5, $MgCl_2$ 1.2, NaH_2PO_4 1.2, $NaHCO_3$ 25 and glucose 11) saturated with 95% O_2 – 5% CO_2, and maintained at 36 ± 1°C. Blind whole-cell voltage-clamp recordings were made from SG neurons (Yoshimura and Nishi 1993). The patch pipettes were filled with a solution (composition in mmol/L: potassium gluconate 136, KCl 5, $CaCl_2$ 0.5, $MgCl_2$ 2, EGTA 5, HEPES 5 and MgATP 5). The tip resistance of the patch pipette was 8–12 MΩ. In the voltage-clamp mode, the holding potentials (V_H) were −70 mV. Stimuli (duration, 100 μs) to elicit EPSCs were given to the dorsal root at a frequency of 0.2 Hz via a suction electrode. The Aδ- or C-afferent-mediated responses evoked by the dorsal root stimulation were distinguished on the basis of the conduction velocity (CV) of the afferent fibers (C, < 0.8 m/s; Aδ, 2–11 m/s) and stimulus threshold (C, >300 μA; Aδ, 40–200 μA), as previously described (Yoshimura and Jessell 1989). The CV was calculated from the latency of the synaptic responses from a stimulus artifact and the length of the dorsal root. The Aδ-afferent-mediated EPSCs were considered to be monosynaptic in nature when the latency remained constant and there was no failure during repetitive stimulation at 20 Hz for 1 s. The C-afferent-mediated EPSCs were considered to be monosynaptic when failures did not occur during stimulation at 2 Hz for 10 s (Nakatsuka *et al.* 1999, 2000). Signals were acquired with a patch clamp amplifier (Axopatch 200B, Molecular Devices, Union City, CA, USA). The data were digitized with an analog-to-digital converter (Digidata 1321 A, Molecular Devices) and analyzed using a special software package (Clampfit version 10.0). mcPAF was applied by perfusion via a three-way stopcock without any change in the perfusion rate or the temperature.

Immunohistochemistry

The anesthetized mice were perfused transcardially with 20 mL of phosphate-buffered saline followed by 50 mL of ice-cold 4% paraformaldehyde 3 min after intraplantar injection with 5% formalin. The L4/5 segments of the DRG were removed, post-fixed in the same fixative, and placed in 30% sucrose for 24 h at 4°C. L4/5 DRG or L5 spinal cord sections (30 μm) attached on a slide-glass were incubated in a blocking solution (3% normal goat serum) and then incubated with anti-phospho-ERK (1 : 200, Cell Signaling, Beverly, MA, USA), anti-TRPV1 (1 : 200, Oncogene, San Diego, CA, USA) or anti-NeuN (1:200, Chemicon, Temecula, CA, USA) for 48 h at 4°C. After washing, tissue sections were incubated with anti-rabbit IgG conjugated Alexa Fluor™ 488 (1 : 1000, Molecular Probes, Eugene, OR, USA) for 3 h at 22–24°C. The sections were analyzed using a LSM510 Imaging System (Zeiss, Oberkochen, Germany). Three to four sections of the L4 DRG from each genotypes ($n = 4$) were selected randomly. The number of phospho-ERK-positive neuronal profiles that showed distinctive phospho-ERK labeling compared with background labeling in DRG sections was counted and was divided by the total number of neurons, and the percentage of immunoreactive neuron profiles was obtained. For the size-frequency analyses, measurement of the cross-sectional areas of TRPV1 immunoreactive-positive neurons (wild type: 418 cells, *pafr*−/−: 330 cells) was made by using an LSM Image Browser (Zeiss) and only neurons with clearly visible nuclei were used for the quantification.

Statistical analyses

Analysis of the time-course of the duration of licking and biting response was performed by two factors (group × times) repeated measures analysis of variance (ANOVA). The other results were evaluated using the Student's *t*-test or Mann-Whitney *U*-test.

Results

Acute pain behaviors in *pafr*−/− mice

To examine the sensitivities to acute physiological pain, the withdrawal responses from the noxious range of radiant heat and mechanical stimuli by von Frey filaments were measured in both wild-type and *pafr*−/− mice. In the tail-flick test, the latencies to flick their tail from heat at both 30 and 50 V were not different between wild-type and *pafr*−/− mice (Fig. 1a). The latency to withdraw their hindpaw from heat was not altered at 50 V, but was slightly increased at 30 V in *pafr*−/− mice ($p < 0.05$, Fig. 1b). In a test of mechanical pain, *pafr*−/− mice were indistinguishable from wild-type mice in the paw withdrawal threshold (Fig. 1c).

We subsequently tested the effect of PAFR ablation on chemical-induced cutaneous pain behaviors evoked by intraplantar injection of capsaicin, an activator of transient receptor potential vanilloid type 1 (TRPV1) channel which is expressed in nociceptors (Caterina and Julius 2001). Wild-type mice exhibited intense licking and biting responses to the injected hindpaw, but *pafr*−/− mice spent

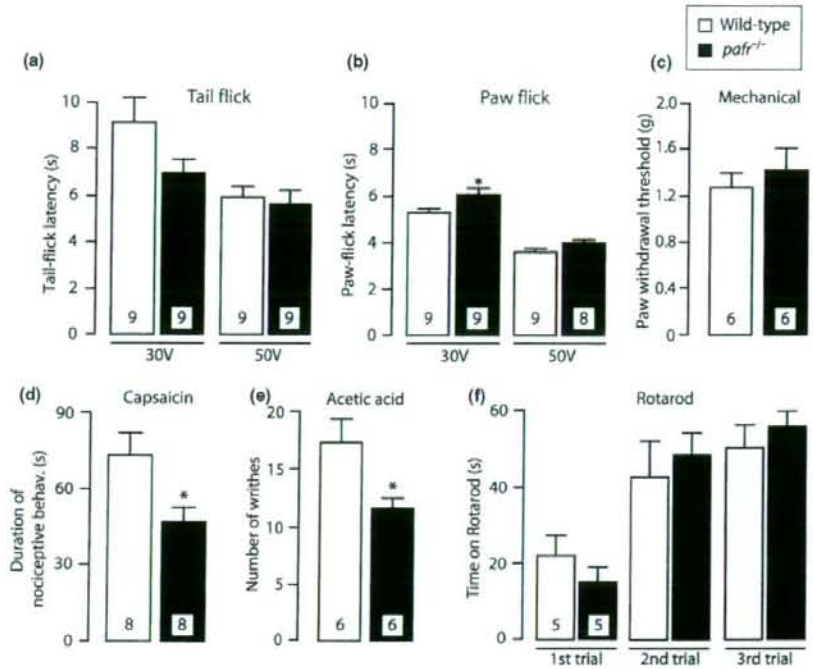

Fig. 1 Acute thermal and mechanical pain and chemical-induced pain in *pafr*−/− mice. (a and b) Tail-flick and paw-flick tests, respectively. Values represent the latency (s) to tail or paw flick from the heat source. $^*p < 0.05$ versus wild-type. (c) Mechanical pain test. Values indicate the threshold (g) to elicit paw withdrawal behavior in response to noxious mechanical stimuli. (d) Capsaicin test. Capsaicin (1.6 μg/20 μL) was injected intraplantarly into the hindpaw. Values represent the duration of licking and biting responses measured for 5 min after the injection. $^*p < 0.05$ versus wild-type. (e) Visceral pain in response to acetic acid (0.8%). Values represent the number of abdominal stretches (writhes). $^*p < 0.05$ versus wild-type. (f) Rotarod performance test. Values represent the duration (s) that mice remain on the rotating rod measured three times. All data are presented as mean ± SEM of 5–9 mice.

significantly less time licking and biting ($p < 0.05$, Fig. 1d). We also found that abdominal writhing behavior in response to intraperioneal injection with acetic acid, a model of chemical-induced visceral inflammatory pain, was significantly reduced in *pafr*−/− mice ($p < 0.05$, Fig. 1e). A reduction in pain behaviors is occasionally misinterpreted as a result of non-specific motor dysfunction, but the rotarod performance test demonstrated no significant difference in either the time on the rotarod at the first trial or an increase in the time on the rotarod throughout the trials between the two genotypes (Fig. 1f).

Impaired tissue injury-induced pain behavior in *pafr*−/− mice

To determine the role of PAFR in tissue injury-induced acute and persistent pain, we assessed the pain response following the injection of formalin into the hindpaw. In wild-type mice, injection of formalin elicited biphasic biting and licking behaviors: the first phase started immediately after the injection and lasted for 5 min, and the second phase lasted for 60 min (Fig. 2a). The pattern of biphasic behaviors was not altered in *pafr*−/− mice, but the magnitude was significantly reduced ($F_{1,12} = 2.703$, $p < 0.01$) (Fig. 2a). A significant difference was observed during 0–5 min (first phase, $p < 0.01$) and during 25–35 min ($p < 0.05$) after the injection (Fig. 2a). *pafr*−/− mice displayed a significant reduction to 35% of the pain response during 10–35 min in the second phase after the injection of formalin ($p < 0.05$, Fig. 2b). The second phase is related to the hyperexcitability of primary afferent neurons in response to inflammation, but the degree of formalin-induced swelling of the injected hindpaw, as indicated by an increase in the weight of the hindpaw 60 min after the injection, was not significantly different between the two genotypes (Fig. 2c). Our data show that PAFR has a crucial role in the modulation of injury-induced pain.

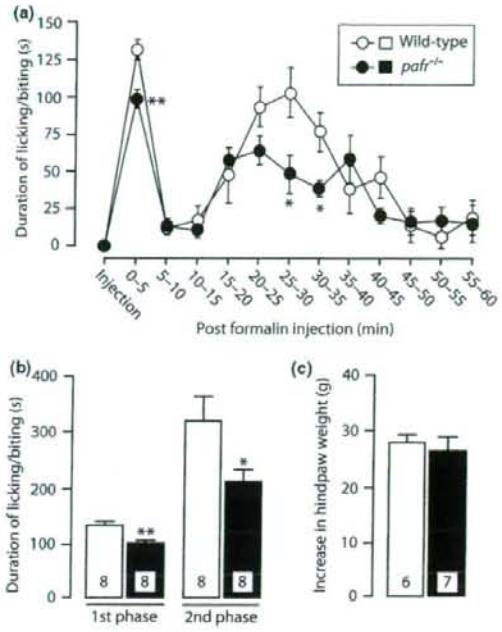

Fig. 2 Impaired pain behavior following tissue injury by formalin in *pafr*–/– mice. (a and b) Formalin pain. Mice were injected intraplantarly with formalin (5%). Values represent the duration (s) of licking and biting responses for each 5-min interval (a), from 0 to 5 min (first phase) and for 10–35 min (second phase) (b), and the change in the weight of the hindpaw 60 min after the injection of formalin (5%) or PBS (c). $^{*}p < 0.05$, $^{**}p < 0.01$ versus wild-type. All data are presented as mean ± SEM of 6–8 mice.

Histological characterization of dorsal root ganglion neurons in *pafr*–/– mice

To investigate whether the lack of PAFR alters cytoarchitectural and neurochemical properties in DRG neurons, we measured the cross-sectional areas of total and TRPV1-positive (TRPV1+) DRG neurons with clearly visible nuclei and analyze their size frequency distributions. As shown in Fig. 3a, no alterations were observed in the size frequency and the mean somal area of total DRG neurons between wild-type (446.4 $\mu m^2 \pm 31.3$) and *pafr*–/– mice (468.1 $\mu m^2 \pm 16.1$). In wild-type mice, TRPV1 immunoreactivity was observed predominantly in small-sized neurons (mean somal area: 203.9 $\mu m^2 \pm 1.3$) and the percentage of TRPV1+ neurons was 34.3% of total DRG neurons (Fig. 3b). The mean somal area (197.0 $\mu m^2 \pm 2.4$) and percentage (35.0%) in the DRG of *pafr*–/– mice was similar to those of wild-type mice. Furthermore, TRPV1 immunoreactivities in the dorsal horn of both wild-type and *pafr*–/– mice were localized in the superficial lamina (Fig. 3c). In addition, there was no clear difference in the

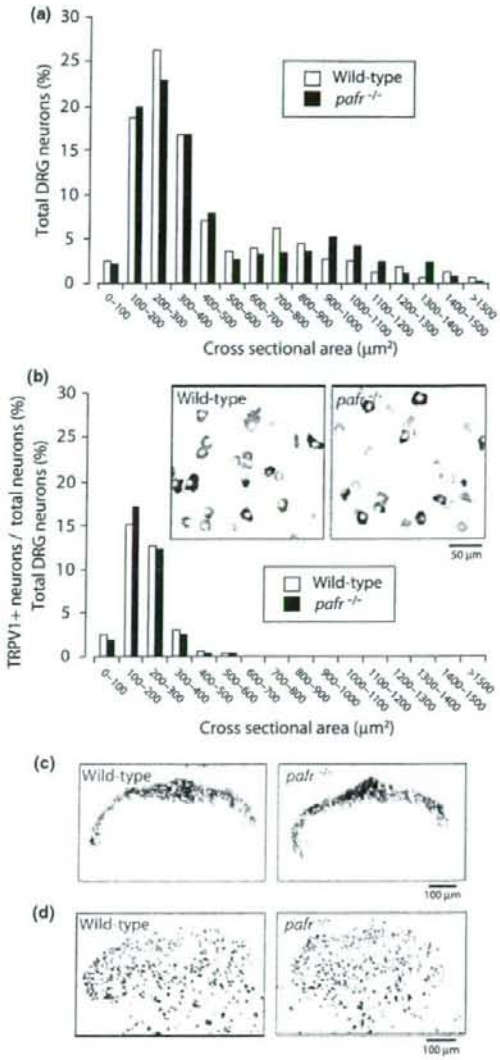

Fig. 3 Cytoarchitectural and neurochemical properties in dorsal root ganglion (DRG) neurons in *pafr*–/– mice. (a and b) Size-frequency histogram illustrating the distribution of the cross-sectional areas of total (a) and TRPV1-positive (b) DRG neurons of wild-type and *pafr*–/– mice. Inset photographs in the panel (b) showing TRPV1 immunoreactivity in the DRG of both strains. Scale bar: 50 μm. (c and d) Immunoreactivities of TRPV1 (c) and NeuN (d) in the dorsal horn of wild-type and *pafr*–/– mice. Scale bar: 100 μm.

immunoreactivity or localization of the neuronal marker NeuN in the dorsal horn between both strains (Fig. 3d). These observations suggest that wild-type and *pafr*–/–

mice have similar cytoarchitectural and neurochemical properties in DRG neurons.

PAF receptor agonist-evoked intracellular Ca^{2+} responses in dorsal root ganglion neurons

Activating PAFR causes Ca^{2+} mobilization through stimulating the G-protein/phospholipase C/IP_3 pathway (Ishii and Shimizu 2000; Honda *et al.* 2002). To examine whether functional PAFR are expressed, we monitored changes in the level of intracellular Ca^{2+} ($[Ca^{2+}]_i$) following an application of methylcarbamyl PAF (mcPAF), a PAFR agonist, in individual DRG neurons. We first applied 75 mmol/L KCl to distinguish neuronal cells. In the DRG neuronal cells (n = 193 cells), mcPAF (1 μmol/L) produced an increase in the 340/360 emission ratio for fura-2 (n = 21 cells) (Fig. 4), indicating that activating PAFR caused an increase in $[Ca^{2+}]_i$ in a subset of DRG neurons. Interestingly, most of the mcPAF-sensitive DRG neurons also responded to capsaicin (1 μmol/L) (n = 18). Moreover, in capsaicin-sensitive DRG neurons from wild-type mice, mcPAF also produced an increase in $[Ca^{2+}]_i$ (5 of 37 cells tested), which was not observed in *pafr*−/− mice (0 of 41 cells tested). These results indicate the presence of functional PAFR in DRG neurons that appear to be nociceptors.

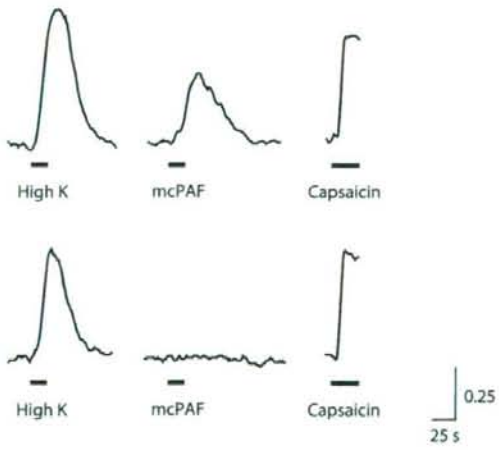

Fig. 4 Ca^{2+} response in individual primary afferent sensory neurons by PAF receptor (PAFR) agonist. Intracellular Ca^{2+} imaging analysis using the Ca^{2+}-sensitive fluorescent dye fura-2 was performed. The traces show KCl (75 mmol/L, 5 s)-evoked a transient increase in the 340/360 emission ratio for fura-2 in acute dissociated dorsal root ganglion (DRG) neurons (n = 193 cells). In 193 DRG neurons, 21 neurons showed an increase in the ratio when applying methylcarbamyl PAF (mcPAF: 1 μmol/L, 10 s) (upper). The other cells (n = 172) did not respond (lower). Most of the mcPAF-responsive DRG neurons (n = 18) also showed an increase in the ratio by capsaicin (1 μmol/L).

Roles of PAF receptor on synaptic transmission in spinal dorsal horn neurons and spinal pain behaviors

Activation of primary afferent sensory neurons causes the release of neurotransmitters in the dorsal horn. To examine whether PAFR has a role in modulating synaptic transmission in the dorsal horn, we recorded dorsal root stimulation-evoked EPSCs in substantia gelatinosa (SG) neurons where primary afferent terminals terminate, using spinal cord slices with attached dorsal roots. Stimulation of the dorsal root always evoked EPSCs with monosynaptic Aδ- and C-afferent properties (Fig. 5a). The CVs of Aδ- and C-afferent fibers for those recordings were 6.4 ± 1.1 and 0.6 ± 0.1 m/s (Fig. 5a), within the range of Aδ- and C-afferent fiber CVs, respectively (Yoshimura and Jessell 1989). The bath application of mcPAF (30 and 60 μmol/L) for 1 min did not alter the amplitude of the Aδ- and C-evoked EPSCs in SG neurons (Fig. 5b).

Glutamate and substance P are major neurotransmitters released from primary sensory neurons in the dorsal horn and activate NMDA receptors and tachykinin NK_1 receptors on dorsal horn neurons, respectively (Nichols *et al.* 1999; South *et al.* 2003). We thus examined whether PAFR deletion

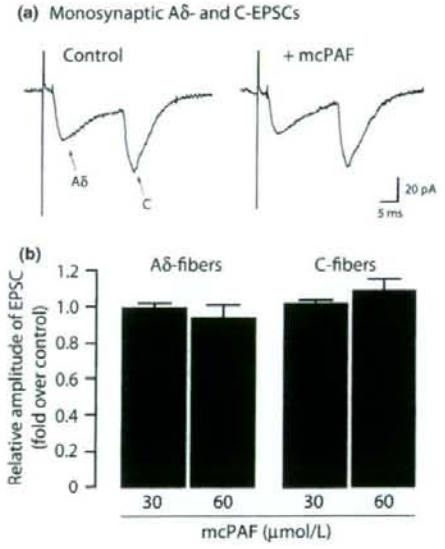

Fig. 5 Effect of PAF receptor (PAFR) agonist on glutamatergic excitatory post-synaptic currents (EPSCs) in substantia gelatinosa (SG) neurons by stimulating the dorsal roots. (a) Traces of monosynaptic Aδ- and C-fibers before (control) and just after the treatment with methylcarbamyl PAF (mcPAF: 30 and 60 μmol/L, 1 min) (+mcPAF). (b) Peak amplitudes of monosynaptic Aδ- and C-fiber-evoked EPSCs under the action of mcPAF, relative to those in the control. V_H = −70 mV. The data are presented as mean ± SEM of 3–11 SG neurons.

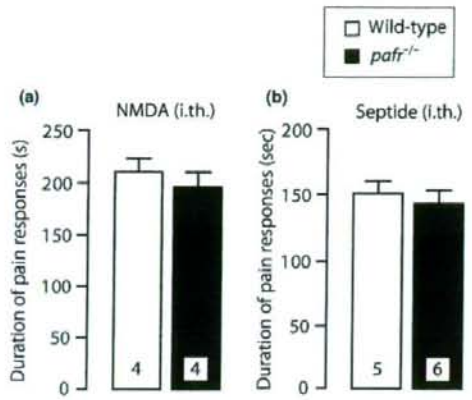

Fig. 6 Spinal pain evoked by intrathecal administration of agonists for NMDA and NK_1 receptors (a and b). Mice were injected intrathecally with NMDA (0.2 μg/5 μL) (a) or septide (10 μg/5 μL) (b). Values indicate the duration (s) of pain responses (licking, biting, and scratching) for 5 min after the injection. All data are presented as mean ± SEM of 4–6 mice.

affected the NMDA and NK_1 receptor-mediated pain responses. Administering intrathecally NMDA (0.2 μg/5 μL) and septide (10 μg/5 μL), an agonist for NK_1, to wild-type mice both produced biting, licking, and scratching behaviors (Fig. 6a and b). The duration of pain responses was altered in *pafr*−/− mice neither by NMDA nor by septide (Fig. 6a and b). These results indicate a minor role of PAFR in pain processing in the spinal dorsal horn under a normal condition.

Reduced ERK activation in DRG neurons following tissue injury in *pafr*−/− mice

As noted above, *pafr*−/− mice displayed a reduction in the persistent phase of tissue injury pain. We investigated the role of PAFR in the activation of ERK in primary sensory neurons, which is an important kinase in sensitization and therefore in persistent pain (Dai *et al.* 2002; Obata and Noguchi 2004; Zhuang *et al.* 2004). Activated ERK was detected by immunofluorescence labeling with an antibody for recognizing phosphorylated ERK (phospho-ERK). In the DRG from wild-type mice after intraplantar injection of formalin, phospho-ERK-positive neurons were observed in 8% of total DRG neurons (82/947 cells, Fig. 7a, c). By contrast, the numbers of phospho-ERK-positive neurons in the DRG from *pafr*−/− mice after formalin injection were significantly fewer, and the percentage of cells positive to phospho-ERK was decreased to 3% of total cells ($p < 0.05$) (39/1204 cells, Fig. 7b, c). Our data suggest that PAFR is required for the ERK activation in primary afferent sensory neurons following tissue injury.

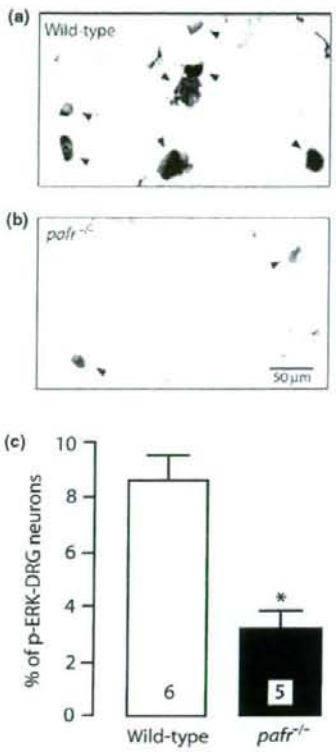

Fig. 7 Reduced extracellular signal-related protein kinase (ERK) activation in primary sensory neurons by tissue injury in *pafr*−/− mice. (a and b) Photographs of phospho-ERK-immunostained L4/5 DRG section of wild-type (a) and *pafr*−/− mice (b) 3 min after injection of formalin (5%). Scale bar: 50 μm. (c) The percentage of phospho-ERK-positive neurons (arrowheads in a and b) in the total neurons counted. *$p < 0.05$ versus wild-type. The data are presented as mean ± SEM of 5–6 mice.

To determine the functional relevance of ERK activation to the tissue injury-induced pain behavior, we injected the selective MEK inhibitor U0126 into rats through a catheter whose tip was positioned near the L5 DRG and examined its effect on the formalin-induced pain behaviors. In this experiment, we used rats in order to apply U0126 preferentially to the L5 DRG rather than to the L5 spinal cord. The pattern of biphasic behaviors was almost similar between both groups (Fig. 8a). U0126 did not alter the duration of the first phase (Fig. 8b), but the duration of the second phase of the pain response was significantly suppressed by the pretreatment with U0126 ($p < 0.05$, Fig. 8b) as compared with vehicle-treated rats. These results indicate that ERK activation is important in the expression of the persistent phase of formalin-induced pain behavior.

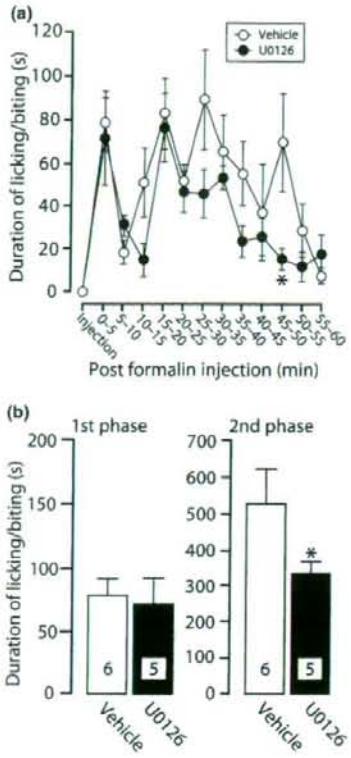

Fig. 8 Reduced persistent phase of formalin-induced pain behavior by pretreatment with U0126. (a) Values represent the duration (s) of licking and biting responses for each 5-min interval (a). (b) The sums of the durations of the formalin-induced biting and licking response during first phase (0–5 min; left) and second phase (10–60 min, right) after 2% formalin injection. The mitogen-activated protein kinase kinase (MEK) inhibitor U0126 (20 nmol/10 μL) was injected through a catheter whose tip was positioned near the L5 DRG 10 min before the formalin injection. $^*p < 0.05$ versus vehicle-treated group. Each point and column represents the mean ± SEM of 5–6 rats.

Discussion

To reveal the precise role of PAFR in pain signaling, we employed a series of pain tests using mice lacking PAFR and found that *pafr*−/− mice exhibited impaired persistent pain behaviors resulting from tissue injury by locally injecting formalin at the periphery without any non-specific motor dysfunction. *pafr*−/− mice also showed a reduction of the acute pain behaviors that are evident in formalin injury-induced pain, capsaicin-induced cutaneous pain and acetic acid-induced visceral pain. By contrast, the behavioral responses to brief noxious thermal and mechanical stimulation in *pafr*−/− mice were comparable to those of wild-type littermates. These results thus indicate that *pafr*−/− mice do not show alterations in all forms of pain responses but rather exhibit aberrant phenotypes in specialized pain states.

It appeared that the acute pain behaviors that were reduced in *pafr*−/− mice were related to nociceptor stimulation. Capsaicin stimulates nociceptors via the activation of TRPV1 channels (Caterina and Julius 2001), and the acute phase of formalin pain is also related to the direct stimulation of nociceptors by formalin (Tjolsen *et al.* 1992; McCall *et al.* 1996; Puig and Sorkin 1996). However, *pafr*−/− mice showed no alteration in their responses to brief noxious stimulation. Although one possibility is that the lack of PAFR may alter cytoarchitectural and neurochemical properties of DRG neurons, we did not observe any changes in the size-frequency distribution and the mean cell area of either total or TRPV1-positive DRG neurons between wild-type and *pafr*−/− mice. One of the differences in these pain tests was the duration of nociceptors stimulation. Indeed, excitation of C-fibers is observed at least for 2–3 min after the injection of formalin (McCall *et al.* 1996; Puig and Sorkin 1996), which is much longer than that from applying noxious thermal stimuli (less than 10 s; Fig. 1). Thus, the PAF/PAFR system may become active in response to a relatively prolonged stimulation of nociceptors. Although the reduced pain behaviors in the first phase of formalin pain in *pafr*−/− mice conflicts with the data of a previous work showing that PAFR antagonists did not suppress the first phase (Teather *et al.* 2002), this might be explained by the pharmacological non-specificity of PAFR antagonists (Kondratskaya *et al.* 2002) and by the difference in the experimental procedures (the indicator of the pain response and the concentration of formalin).

Our Ca^{2+} imaging study showing that a PAFR agonist produced a Ca^{2+} response in capsaicin-sensitive DRG neurons, presumably through stimulating the G-protein/phospholipase C/IP_3 pathway (Ishii and Shimizu 2000; Honda *et al.* 2002), suggests the presence of functional PAFR in nociceptors. This notion is supported by previous data that PAFR mRNA is detected in the DRG (Morita *et al.* 2004) and that a PAFR agonist induces gene expression in primary sensory neurons (Nakasaki *et al.* 1999). However, we observed no alterations in the afferent-evoked EPSCs in SG neurons by PAFR agonist nor in spinal pain behaviors between wild-type and *pafr*−/− mice, suggesting that PAFR has a minor role in excitatory synaptic transmission in SG neurons. This is apparently in contrast to previous data showing that intrathecal administration of PAF produces hypersensitivity to innocuous mechanical stimuli (tactile allodynia), which is mediated by glutamate receptors in the spinal cord (Morita *et al.* 2004). It is conceivable that activating PAFR may modulate synaptic transmission in dorsal horn neurons other than SG neurons, which could be involved in tactile allodynia caused by intrathecal administration of PAF. At the periphery, local injection of PAFR

agonist has been demonstrated not to produce spontaneous pain behaviors (e.g., licking or biting response) (Wheeler-Aceto *et al.* 1990) but rather to enhance the sensitivities to noxious stimuli (Bonnet *et al.* 1981; Belanger *et al.* 1987; Dallob *et al.* 1987). PAF is released from keratinocytes (Alappatt *et al.* 2000) and inflammatory cells, such as neutrophils, eosinophils, monocytes/macrophages, and vascular endothelial cells (Montrucchio *et al.* 2000). The level of PAF is indeed increased in inflamed peripheral tissue (Noguchi *et al.* 1989; Doi *et al.* 2006). These results together suggest that a lack of the PAF/PAFR system of primary afferent sensory neurons may be responsible for the reduced pain behaviors, especially by tissue injury, in *pafr*−/− mice.

An important finding in the present study is that PAFR plays a role in the activation of ERK in the primary sensory neurons as well as in persistent pain behaviors following peripheral tissue injury. ERK has recently received attention as an intracellular event generating sensitization of primary sensory neurons to peripheral inputs (Dai *et al.* 2002; Obata and Noguchi 2004; Zhuang *et al.* 2004). The persistent phase of formalin pain that was attenuated in *pafr*−/− mice (Fig. 2a, b) has been considered to be associated in part with the hyperexcitability of primary sensory neurons at the inflamed site induced by formalin (McCall *et al.* 1996; Puig and Sorkin 1996; Pitcher and Henry 2002). We also found that the formalin-induced persistent pain was suppressed by the MEK inhibitor U0126 administered near the L5 DRG where is a very long distance away from the L5 spinal cord. These data suggest that the impairment in the persistent pain behaviors in *pafr*−/− mice may be associated with the reduced tissue injury-induced ERK activation in cell bodies of primary sensory neurons in the DRG, although we can not exclude a possible involvement of ERK in dorsal horn neurons (Ji *et al.* 1999) or central afferent terminals in the suppressing effect of U0126. Additionally, an alteration of the gene expression by ERK (Obata and Noguchi 2004) suggests the possibility that PAFR may also play a role in more long-term adaptive changes following tissue injury.

The reduction in the proportion of phosphorylated ERK-positive DRG neurons (about 5%) in *pafr*−/− mice was slightly lower than that of mcPAF-responded DRG neurons that had been acutely dissociated from the DRG (about 10 % of DRG neurons tested). Considering the fact that L4/5 DRG neurons projects their fibers not only to the plantar area of the hindpaw but also to other targets, such as the viscera, muscle and skin of other areas (Thornton *et al.* 2005), a subpopulation of PAFR-expressing DRG neurons may project to the plantar surface and be associated with ERK activation in response to tissue injury by formalin.

The mechanisms underlying the ERK activation in sensory neurons by PAFR remain unclear, but several possibilities are considered. Our present data showing that lacking PAFR reduced ERK activation in DRG neurons that occurred shortly after formalin injection suggest the possibility that activating PAFR by PAF presumably released at the periphery in response to tissue injury may increase signals that lead to ERK activation in cell bodies of DRG neurons such as the action potentials (Fields *et al.* 1997; Dai *et al.* 2002) or the TRPV1 channel activity (Dai *et al.* 2002) at the periphery. Alternatively, since the PAF level is increased in inflamed tissue (Noguchi *et al.* 1989; Kihara *et al.* 2005; Doi *et al.* 2006). PAF (or coordinated with other chemical mediators) may produce a direct activation of ERK at peripheral nerve endings, which has been implicated in causing peripheral sensitization (Dai *et al.* 2002), and may secondary activate ERK in cell bodies of DRG neurons. Indeed, a subset of DRG neurons has been reported to activate ERK by stimulating G protein-coupled receptors (Aley *et al.* 2001), and PAFR stimulation causes the phosphorylation of ERK in various cells (Ishii and Shimizu 2000; Honda *et al.* 2002).

Tissue-damaging stimuli generate a complex cascade of transmitters and modulators at the periphery, which in turn develop tissue injury-induced persistent pain (Julius and Basbaum 2001). The present findings obtained from mice lacking PAFR have now provided evidence that PAFR signaling activated by endogenous PAF may be an important event in producing persistent pain and ERK activation in primary sensory neurons after peripheral tissue injury.

Acknowledgements

This work was supported by grants from the Ministry of Education, Culture, Sports, Science and Technology of Japan (to MT, KI).

References

Adachi T., Aoki J., Manya H., Asou H., Arai H. and Inoue K. (1997) PAF analogues capable of inhibiting PAF acetylhydrolase activity suppress migration of isolated rat cerebellar granule cells. *Neurosci. Lett.* **235**, 133–136.

Alappatt C., Johnson C. A., Clay K. L. and Travers J. B. (2000) Acute keratinocyte damage stimulates platelet-activating factor production. *Arch. Dermatol. Res.* **292**, 256–259.

Aley K. O., Martin A., McMahon T., Mok J., Levine J. D. and Messing R. O. (2001) Nociceptor sensitization by extracellular signal-regulated kinases. *J. Neurosci.* **21**, 6933–6939.

Archer C. B., Page C. P., Paul W., Morley J. and MacDonald D. M. (1984) Inflammatory characteristics of platelet activating factor (PAF-acether) in human skin. *Br. J. Dermatol.* **110**, 45–50.

Basran G. S., Page C. P., Paul W. and Morley J. (1984) Platelet-activating factor: a possible mediator of the dual response to allergen? *Clin. Allergy* **14**, 75–79.

Belanger P., Maycock A., Guindon Y. *et al.* (1987) L-656,224 (7-chloro-2-[(4-methoxyphenyl)methyl]-3- methyl-5-propyl-4-benzofuranol): a novel, selective, orally active 5-lipoxygenase inhibitor. *Can. J. Physiol. Pharmacol.* **65**, 2441–2448.

Bonnet J., Loiseau A. M., Orvoen M. and Bessin P. (1981) Platelet-activating factor acether (PAF-acether) involvement in acute inflammatory and pain processes. *Agents Actions* **11**, 559–562.

Caterina M. J. and Julius D. (2001) The vanilloid receptor: a molecular gateway to the pain pathway. *Annu. Rev. Neurosci.* **24**, 487–517.

Dai Y., Iwata K., Fukuoka T., Kondo E., Tokunaga A., Yamanaka H., Tachibana T., Liu Y. and Noguchi K. (2002) Phosphorylation of extracellular signal-regulated kinase in primary afferent neurons by noxious stimuli and its involvement in peripheral sensitization. *J. Neurosci.* **22**, 7737–7745.

Dallob A., Guindon Y. and Goldenberg M. M. (1987) Pharmacological evidence for a role of lipoxygenase products in platelet-activating factor (PAF)-induced hyperalgesia. *Biochem. Pharmacol.* **36**, 3201–3204.

Doi K., Okamoto K., Negishi K. *et al.* (2006) Attenuation of folic acid-induced renal inflammatory injury in platelet-activating factor receptor-deficient mice. *Am. J. Pathol.* **168**, 1413–1424.

Dupre D. J., Le Gouill C., Rola-Pleszczynski M. and Stankova J. (2001) Inverse agonist activity of selected ligands of platelet-activating factor receptor. *J. Pharmacol. Exp. Ther.* **299**, 358–365.

Fields R. D., Eshete F., Stevens B. and Itoh K. (1997) Action potential-dependent regulation of gene expression: temporal specificity in Ca^{2+}, cAMP-responsive element binding proteins, and mitogen-activated protein kinase signaling. *J. Neurosci.* **17**, 7252–7266.

Honda Z., Nakamura M., Miki I. *et al.* (1991) Cloning by functional expression of platelet-activating factor receptor from guinea-pig lung. *Nature* **349**, 342–346.

Honda Z., Ishii S. and Shimizu T. (2002) Platelet-activating factor receptor. *J. Biochem. (Tokyo)* **131**, 773–779.

Huang S. H., Duke R. K., Chebib M., Sasaki K., Wada K. and Johnston G. A. (2004) Ginkgolides, diterpene trilactones of *Ginkgo biloba*, as antagonists at recombinant $\alpha_1\beta_2\gamma_{2\,L}$ $GABA_A$ receptors. *Eur. J. Pharmacol.* **494**, 131–138.

Ishii S. and Shimizu T. (2000) Platelet-activating factor (PAF) receptor and genetically engineered PAF receptor mutant mice. *Prog. Lipid Res.* **39**, 41–82.

Ishii S., Kuwaki T., Nagase T. *et al.* (1998) Impaired anaphylactic responses with intact sensitivity to endotoxin in mice lacking a platelet-activating factor receptor. *J. Exp. Med.* **187**, 1779–1788.

Ivic L., Sands T. T., Fishkin N., Nakanishi K., Kriegstein A. R. and Stromgaard K. (2003) Terpene trilactones from Ginkgo biloba are antagonists of cortical glycine and $GABA_A$ receptors. *J. Biol. Chem.* **278**, 49279–49285.

Ji R. R., Baba H., Brenner G. J. and Woolf C. J. (1999) Nociceptive-specific activation of ERK in spinal neurons contributes to pain hypersensitivity. *Nat. Neurosci.* **2**, 1114–1119.

Julius D. and Basbaum A. I. (2001) Molecular mechanisms of nociception. *Nature* **413**, 203–210.

Kihara Y., Ishii S., Kita Y., Toda A., Shimada A. and Shimizu T. (2005) Dual phase regulation of experimental allergic encephalomyelitis by platelet-activating factor. *J. Exp. Med.* **202**, 853–863.

Koizumi S., Watano T., Nakazawa K. and Inoue K. (1994) Potentiation by adenosine of ATP-evoked dopamine release via a pertussis toxin-sensitive mechanism in rat phaeochromocytoma PC12 cells. *Br. J. Pharmacol.* **112**, 992–997.

Kondratskaya E. L., Lishko P. V., Chatterjee S. S. and Krishtal O. A. (2002) BN52021, a platelet activating factor antagonist, is a selective blocker of glycine-gated chloride channel. *Neurochem. Int.* **40**, 647–653.

Mayer R. A., Ringkamp M., Campbell J. N. and McMahon S. B. (2006) *Peripheral Mechanisms of Cutaneous Nociception*, 5th Edn, pp 3–34. Elsevier, Churchill-Livingstone.

McCall W. D., Tanner K. D. and Levine J. D. (1996) Formalin induces biphasic activity in C-fibers in the rat. *Neurosci. Lett.* **208**, 45–48.

Merlos M., Giral M., Balsa D., Ferrando R., Queralt M., Puigdemont A., Garcia-Rafanell J. and Forn J. (1997) Rupatadine, a new potent, orally active dual antagonist of histamine and platelet-activating factor (PAF). *J. Pharmacol. Exp. Ther.* **280**, 114–121.

Montrucchio G., Alloatti G. and Camussi G. (2000) Role of platelet-activating factor in cardiovascular pathophysiology. *Physiol. Rev.* **80**, 1669–1699.

Morita K., Morioka N., Abdin J., Kitayama S., Nakata Y. and Dohi T. (2004) Development of tactile allodynia and thermal hyperalgesia by intrathecally administered platelet-activating factor in mice. *Pain* **111**, 351–359.

Nakasaki T., Masuyama K., Fukui H., Ogino S., Eura M., Samejima Y., Ishikawa T. and Yumoto E. (1999) Effects of PAF on histamine H1 receptor mRNA expression in rat trigeminal ganglia. *Prostaglandins Other Lipid Mediat.* **58**, 29–41.

Nakatsuka T., Park J. S., Kumamoto E., Tamaki T. and Yoshimura M. (1999) Plastic changes in sensory inputs to rat substantia gelatinosa neurons following peripheral inflammation. *Pain* **82**, 39–47.

Nakatsuka T., Ataka T., Kumamoto E., Tamaki T. and Yoshimura M. (2000) Alteration in synaptic inputs through C-afferent fibers to substantia gelatinosa neurons of the rat spinal dorsal horn during postnatal development. *Neuroscience* **99**, 549–556.

Nichols M. L., Allen B. J., Rogers S. D. *et al.* (1999) Transmission of chronic nociception by spinal neurons expressing the substance P receptor. *Science* **286**, 1558–1561.

Noguchi K., Morita I. and Murota S. (1989) The detection of platelet-activating factor in inflamed human gingival tissue. *Arch. Oral Biol.* **34**, 37–41.

Obata K. and Noguchi K. (2004) MAPK activation in nociceptive neurons and pain hypersensitivity. *Life Sci.* **74**, 2643–2653.

Pitcher G. M. and Henry J. L. (2002) Second phase of formalin-induced excitation of spinal dorsal horn neurons in spinalized rats is reversed by sciatic nerve block. *Eur. J. Neurosci.* **15**, 1509–1515.

Prescott S. M., Zimmerman G. A., Stafforini D. M. and McIntyre T. M. (2000) Platelet-activating factor and related lipid mediators. *Annu. Rev. Biochem.* **69**, 419–445.

Puig S. and Sorkin L. S. (1996) Formalin-evoked activity in identified primary afferent fibers: systemic lidocaine suppresses phase-2 activity. *Pain* **64**, 345–355.

Sakurada T., Wako K., Sugiyama A., Sakurada C., Tan-No K. and Kisara K. (1998) Involvement of spinal NMDA receptors in capsaicin-induced nociception. *Pharmacol. Biochem. Behav.* **59**, 339–345.

South S. M., Kohno T., Kaspar B. K. *et al.* (2003) A conditional deletion of the NR1 subunit of the NMDA receptor in adult spinal cord dorsal horn reduces NMDA currents and injury-induced pain. *J. Neurosci.* **23**, 5031–5040.

Teather L. A., Magnusson J. E. and Wurtman R. J. (2002) Platelet-activating factor antagonists decrease the inflammatory nociceptive response in rats. *Psychopharmacology (Berl)* **163**, 430–433.

Thornton P. D., Gerke M. B. and Plenderleith M. B. (2005) Histochemical localisation of a galactose-containing glycoconjugate expressed by sensory neurones innervating different peripheral tissues in the rat. *J. Peripher. Nerv. Syst.* **10**, 47–57.

Tjolsen A., Berge O. G., Hunskaar S., Rosland J. H. and Hole K. (1992) The formalin test: an evaluation of the method. *Pain* **51**, 5–17.

Tsuda M., Ueno S. and Inoue K. (1999a) In vivo pathway of thermal hyperalgesia by intrathecal administration of alpha,beta-methylene ATP in mouse spinal cord: involvement of the glutamate-NMDA receptor system. *Br. J. Pharmacol.* **127**, 449–456.

Tsuda M., Ueno S. and Inoue K. (1999b) Evidence for the involvement of spinal endogenous ATP and P2X receptors in nociceptive responses caused by formalin and capsaicin in mice. *Br. J. Pharmacol.* **128**, 1497–1504.

Tsuda M., Koizumi S., Kita A., Shigemoto Y., Ueno S. and Inoue K. (2000) Mechanical allodynia caused by intraplantar injection of P2X receptor agonist in rats: involvement of heteromeric $P2X_{2/3}$ receptor signaling in capsaicin-insensitive primary afferent neurons. *J. Neurosci.* **20**, RC90 (1–5).

Tsuda M., Shigemoto-Mogami Y., Koizumi S., Mizokoshi A., Kohsaka S., Salter M. W. and Inoue K. (2003) $P2X_4$ receptors induced in spinal microglia gate tactile allodynia after nerve injury. *Nature* **424**, 778–783.

Wheeler-Aceto H., Porreca F. and Cowan A. (1990) The rat paw formalin test: comparison of noxious agents. *Pain* **40**, 229–238.

Yoshimura M. and Jessell T. M. (1989) Primary afferent-evoked synaptic responses and slow potential generation in rat substantia gelatinosa neurons in vitro. *J. Neurophysiol.* **62**, 96–108.

Yoshimura M. and Nishi S. (1993) Blind patch-clamp recordings from substantia gelatinosa neurons in adult rat spinal cord slices: pharmacological properties of synaptic currents. *Neuroscience* **53**, 519–526.

Zhuang Z. Y., Xu H., Clapham D. E. and Ji R. R. (2004) Phosphatidylinositol 3-kinase activates ERK in primary sensory neurons and mediates inflammatory heat hyperalgesia through TRPV1 sensitization. *J. Neurosci.* **24**, 8300–8309.

Role of platelet-activating factor in pneumolysin-induced acute lung injury

Martin Witzenrath, MD; Birgitt Gutbier; John S. Owen, PhD; Bernd Schmeck, MD; Timothy J. Mitchell, PhD; Konstantin Mayer, MD; Michael J. Thomas, PhD; Satoshi Ishii, PhD; Simone Rosseau, MD; Norbert Suttorp, MD; Hartwig Schütte, MD

Objective: **Acute respiratory failure is a major complication of severe pneumococcal pneumonia, characterized by impairment of pulmonary microvascular barrier function and pulmonary hypertension. Both features can be evoked by pneumolysin (PLY), an important virulence factor of *Streptococcus pneumoniae*. We hypothesized that platelet-activating factor (PAF) and associated downstream signaling pathways play a role in the PLY-induced development of acute lung injury.**

Design: **Controlled, *ex vivo* laboratory study.**

Subjects: **Female Balb/C mice, 8–12 wks old.**

Interventions: **Ventilated and blood-free–perfused lungs of wild-type and PAF receptor–deficient mice were challenged with recombinant PLY.**

Measurements and Main Results: **Intravascular PLY, but not the pneumolysoid Pd-B (PLY with a Trp-Phe substitution at position 433), caused an impressive dose-dependent increase in pulmonary vascular resistance and increased PAF in lung homogenates, as detected by reversed-phase high-performance liquid chromatography coupled to tandem mass spectrometry. The pressor response was reduced in lungs of PAF receptor–deficient mice and after PAF receptor blockade by BN 50730. PLY and exogenous PAF increased thromboxane B2 in lung effluate, and thromboxane receptor inhibition by BM 13505 diminished the pressor response to PLY. Differential inhibition of intracellular signaling steps suggested significant contribution of phosphatidylcholine-specific phospholipase C and protein kinase C and of the Rho/Rho-kinase pathway to PLY-induced pulmonary vasoconstriction. Unrelated to the pulmonary arterial pressor response, microvascular leakage of PLY was diminished in lungs of PAF receptor–deficient mice as well.**

Conclusions: **PAF significantly contributed to PLY-induced acute injury in murine lungs. The PAF-mediated pressor response to PLY depends on thromboxane and on the downstream effectors phosphatidylcholine-specific phospholipase C, protein kinase C, and Rho-kinase. (Crit Care Med 2007; 35:1756–1762)**

Key Words: pneumococcal pneumonia; pneumolysin; acute lung injury; isolated mouse lung; platelet activating factor; thromboxane; Rho-kinase

Community-acquired pneumonia is an important cause of morbidity and mortality. Acute respiratory failure and sepsis are significant complications of severe community-acquired pneumonia and may result in acute respiratory distress syndrome, which is characterized by microvascular leakage and pulmonary hypertension (1). *Streptococcus pneumoniae* is the most prevalent causal pathogen identified in community-acquired pneumonia (2). Pneumolysin (PLY), a cytoplasmic 53-kDa protein toxin, is an important virulence factor of *S. pneumoniae* (3, 4). PLY is produced by all clinical isolates and released during pneumococcal lysis. Bacteremia frequently occurs in pneumococcal pneumonia, and purified human anti-PLY immunoglobulin G protected mice against bacteremic pneumococcal disease and increased survival (5). Moreover, studies with a PLY-negative mutant of *S. pneumoniae* suggested a critical role of PLY in acute pneumococcal sepsis (6). Recently, we observed that intravascular PLY induced hyperpermeability and a massive, rapid, and dose-dependent increase of vascular resistance in isolated mouse lungs (7). These findings provided further evidence that PLY may play an important role in the development of acute lung injury in pneumococcal bacteremia and sepsis. However, the mechanisms contributing to these PLY-induced alterations remain unclear.

Platelet-activating factor (PAF) is a potent lipid mediator implicated in diverse inflammatory disorders, including acute respiratory distress syndrome and sepsis (8). Effects of PAF are exclusively mediated by the PAF receptor (PAF-R), which is expressed in many tissues, including the lungs (9). Pulmonary actions of PAF induce both vascular hyperpermeability and vasoconstriction (8, 10). The present study was designed to test the hypothesis

From the Department of Internal Medicine/Infectious Diseases and Respiratory Medicine, Charité-Universitätsmedizin Berlin, Germany (MW, BG, BS, SR, NS, HS); Department of Biochemistry, Wake Forest University School of Medicine, Winston-Salem, NC (JSO, MJT); Division of Infection and Immunity, Glasgow Biomedical Research Centre, University of Glasgow, UK (TJM); Lung Center, Department of Internal Medicine II, University of Giessen, Germany (KM); and the Department of Biochemistry and Molecular Biology, University of Tokyo, Japan (SI).

The authors have no financial interests to disclose.

Parts of this work contribute to the doctoral thesis of Gutbier.

Supported, in part, by grants from the Bundesministerium für Bildung und Forschung to Drs. Schmeck, Rosseau, and Suttorp (CAPNETZ, Competence Network Community-Acquired Pneumonia).

For information regarding this article, E-mail: hartwig.schuette@charite.de

DOI: 10.1097/01.CCM.0000269212.84709.23

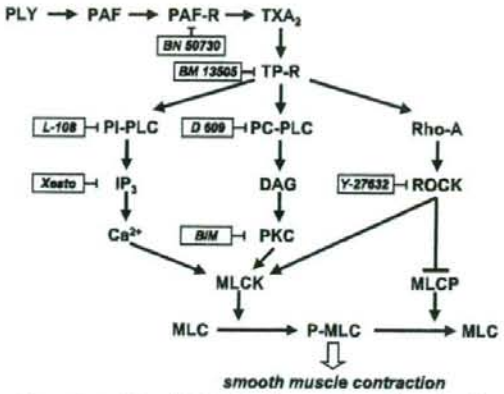

Figure 1. Schematic overview of investigated signaling cascades and employed antagonists. *PLY*, pneumolysin; *PAF*, platelet-activating factor; *PAF-R*, PAF receptor; *TXA_2*, thromboxane A_2; *TP-R*, TXA_2-receptor; *PI-PLC*, phosphatidylinositol-specific phospholipase C; *PC-PLC*, phosphatidylcholine-specific PLC; *IP_3*, inositol trisphosphate; *DAG*, diacylglycerol; *ROCK*, Rho-kinase; *PKC*, protein kinase C; *MLC*, myosin light chain; *MLCK*, MLC kinase; *MLCP*, MLC phosphatase; *P-MLC*, phosphorylated MLC. *BN 50730*, PAF receptor antagonist; *BM 13505*, daltroban, TP-R antagonist; *L-108*, PI-PLC inhibitor; *D 609*, PC-PLC inhibitor; *Xesto*, xestospongin C, inositol trisphosphate antagonist; *BIM*, bisindolylmaleimide, PKC inhibitor; *Y-27632*, ROCK inhibitor.

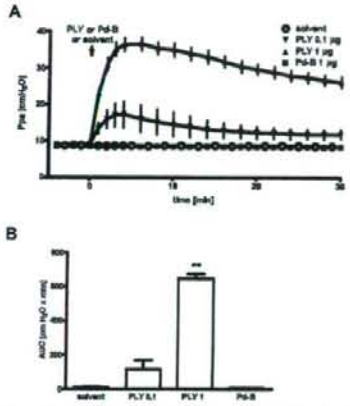

Figure 2. Intravascular pneumolysin (*PLY*), but not Pd-B, induced pulmonary hypertension. PLY (total dose of 0.1 μg or 1.0 μg, respectively), Pd-B (1.0 μg), or solvent were infused via the pulmonary artery within 1 min. *A*, PLY-induced increase of the mean pulmonary arterial pressure (*Ppa*). n = 5 separate experiments per group. *B*, the area under the Ppa curve (*AUC*) markedly increased after PLY but not after Pd-B application. n = 5 per group; $^{**}p < .01$ vs. all other groups.

that PAF and its downstream signaling pathways contribute to PLY-induced impairment of pulmonary hemodynamics and fluid balance.

METHODS

Animals. All animal procedures were approved by the State Office of Health and Social Affairs. PAF-R–deficient mice (PAF-$R^{-/-}$) (11) were backcrossed at least ten times to a Balb/C background. Wild-type (WT) mice were obtained from Charles River (Sulzfeld, Germany).

Isolated Perfused Mouse Lung. Lungs were prepared as described (7, 12), perfused with 37°C sterile Krebs-Henseleit-hydroxyethylamylopectine buffer and ventilated by negative pressure. Pulmonary arterial pressure (Ppa) was continuously monitored. Recombinant PLY, a 53-kDa protein (13), or Pd-B, a mutant PLY protein with a single amino acid substitution at residue number 433 (14), were infused for 1 min into the pulmonary artery or aerosolized into the trachea. For measurement of alveolocapillary permeability, human serum albumin was admixed to the perfusate (0.04%) before toxin application. Bronchoalveolar lavage was performed 30 mins after toxin challenge, and the human serum albumin concentration was measured in bronchoalveolar lavage supernatant (15).

To analyze the role of PAF-related signal transduction pathways in PLY-induced lung injury, we employed different specific inhibitors and antagonists, as summarized in Figure 1. Agents were obtained from the following sources: xestospongin C and L-108 from Biomol (Hamburg, Germany); bisindolylmaleimide, Y-27632, and U46619 from Calbiochem (Darmstadt, Germany); D-609 from Sigma (Deisenhofen, Germany); BM 13505 from Boehringer (Mannheim, Germany); and BN 50730 from Institut Henri Beaufour (Les Ulis, France).

Extraction and Assay of PAF. Lungs were snap frozen 5 mins after PLY infusion, pulverized, weighed, and stored at −80°C. Homogenates were incubated essentially as described (16). Delipidated solids were removed by centrifugation and reserved for total protein assay. After separation (16), the chloroform phase of the solvent was transferred to a fresh tube, and the methanolic phase was washed with 4 mL of chloroform. Both chloroform extracts were pooled, evaporated under a stream of argon, and reconstituted in 1 mL of chloroform/methanol (1:1 vol/vol). Perfusate samples were frozen at −80°C, lipids were extracted in the presence of d3-PAF, and lipid extracts were assayed for total phosphorus and for PAF as described (16). Briefly, PAF was isolated from the lipid extracts by preparative normal-phase high-performance liquid chromatography and quantified using reversed-phase high-performance liquid chromatography coupled to tandem mass spectrometry in the multiple-reaction monitoring mode (16). Delipidated solids from lung homogenates were air-dried, digested, and assayed for total protein, essentially as described (17). The internal standard for PAF measurement, d3-PAF, was synthesized as described (18). Other PAF standards were purchased from Avanti (Alabaster, AL) or from Bachem (King of Prussia, PA).

Thromboxane Quantification. Thromboxane A2 (TXA_2) in perfusion buffer samples was assessed as the stable degradation product TXB_2 by enzyme immunoassay (Cayman Chemicals, Ann Arbor, MI).

Data Analysis. Data are expressed as mean ± SEM. Differences were analyzed by Mann-Whitney U test or one-way analysis of variance followed by *post hoc* Tukey test. All calculations were performed with GraphPad 4 Software (San Diego, CA).

RESULTS

Conserved Undecapeptide Sequence of PLY Accounted for the Pressor Response. Perfusion of isolated WT mice lungs with PLY induced a rapid and dose-dependent Ppa increase (Fig. 1). In contrast, perfusion with the pneumolysoid Pd-B did not alter Ppa (Fig. 2).

PAF and TXA_2 Contributed to PLY-Induced Pulmonary Hypertension. After PLY infusion, PAF content in the venous effluate was below the detection limit. However, in mouse lung tissue, PAF content was significantly increased after PLY infusion (Fig. 3*A*). The PLY-induced Ppa increase was significantly lower in PAF-$R^{-/-}$ compared with WT mice lungs (Fig. 3, *B* and *C*). Baseline Ppa values did not differ between the two groups (WT, 8.83 ± 0.23 cm H_2O; PAF-$R^{-/-}$, 8.30 ± 0.34 cm H_2O), and the dose-dependent vasopressor responses to the thromboxane analogue U46619 did not differ between PAF-$R^{-/-}$ mice and WT mice (maximum delta Ppa to 100 nM U46619: WT, 12.7 ± 0.9 cm H_2O; PAF-$R^{-/-}$, 10.85 ± 2.1 cm H_2O). Moreover, the PAF-R antagonist BN 50730 diminished

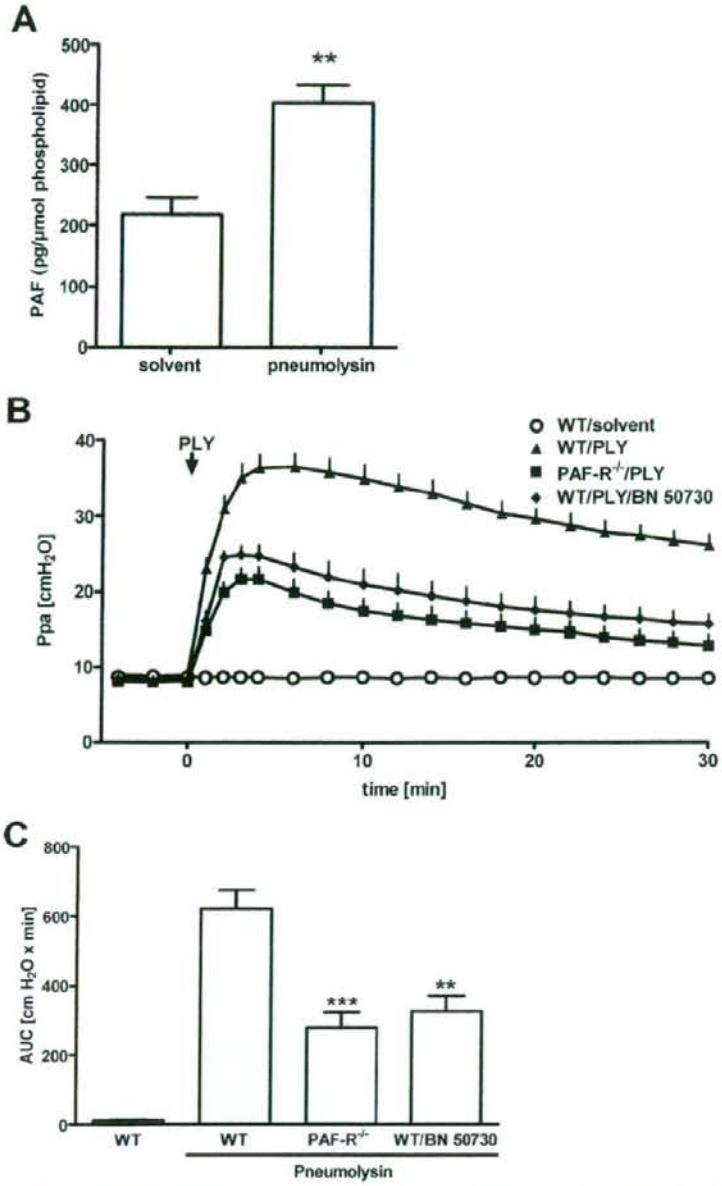

Figure 3. Pulmonary hypertension evoked by pneumolysin (*PLY*) was partly mediated by platelet-activating factor (*PAF*). *A*, PAF was increased in homogenized lung tissue of wild-type (*WT*) mice after PLY infusion as compared with untreated lungs (*solvent*). PAF was measured by reversed-phase high-performance liquid chromatography coupled to tandem mass spectrometry, and PAF levels were related to total lung phospholipids. n = 7 per group; $^{**}p < .01$. *B* and *C*, PLY (1 µg/min) or solvent was infused at t = 0 min for 1 min. Pulmonary arterial pressure (*Ppa*; *B*) and the area under the Ppa curve (*AUC*) values (*C*) were diminished in PLY-challenged lungs of PAF receptor–deficient mice (*PAF-R$^{-/-}$/PLY*) and in WT lungs preperfused with the PAF-R antagonist BN 50730 (10 µM) starting at t = −15 mins (*WT/PLY/BN 50730*) compared with PLY-challenged WT lungs (*WT/PLY*). WT/solvent, n = 5; WT/PLY, n = 8; PAF-R$^{-/-}$/PLY, n = 7; WT/PLY/BN 50730, n = 6. $^{**}p < .01$ vs. WT/PLY; $^{***}p < .001$ vs. WT/PLY.

the pressor response to PLY in lungs of WT mice (Fig. 3, *B* and *C*).

Perfusion of WT mice lungs with PLY induced a significant increase of thromboxane in the venous effluate (Fig. 4*A*). Increase of Ppa and TXA_2 generation was also induced by PAF perfusion (Fig. 4, *A* and *B*). Preperfusion with the specific thromboxane receptor antagonist BM 13505 strongly reduced the PLY-induced pressor response (Fig. 4*C*). A moderate reduction of this pressor response was also observed in lungs preperfused with the 5-lipoxygenase inhibitor AA-861 (10 µM; area under the curve 441.1 ± 49.6 cm H_2O × min, n = 5).

Phosphatidylcholine-Specific Phospholipase C and Protein Kinase C, but Not Phosphatidylinositol-Specific Phospholipase C and Inositol Trisphosphate, Contributed to PLY-Induced Intracellular Signal Transduction. TXA_2 and leukotrienes may contribute to acute pulmonary vasoconstriction via G-coupled receptors linked to phospholipase C (PLC). Pretreatment of perfused lungs with the phosphatidylcholine-specific PLC inhibitor D-609, but not with the phosphatidylinositol-specific PLC inhibitor L-108, largely attenuated the pressor responses to PLY (Fig. 5). Inhibition of the downstream effector of phosphatidylinositol-specific PLC, inositol trisphosphate (IP_3), using the IP_3 receptor antagonist xestospongin C, did not affect PLY-induced vasoconstriction (Fig. 5). In contrast, the selective inhibitor of the phosphatidylcholine-specific PLC downstream effector protein kinase C (PKC), bisindolylmaleimide, largely attenuated PLY-induced vasoconstriction.

Role of Rho-Kinase for PLY-Induced Pressor Response. Inhibition of Rho-kinase by Y-27632 resulted in a distinct reduction of Ppa increase (Fig. 5). Moreover, combined pretreatment with bisindolylmaleimide and Y-27632 had a significantly greater effect than each of the inhibitors and almost completely abolished the PLY-induced vasoconstriction, suggesting an additive role for Rho-kinase besides the PKC pathway.

PAF Contributed to PLY-Induced Hyperpermeability. PLY infusion increased isolated lung permeability (Fig. 6*A*). Moreover, aerosolized PLY evoked lung hyperpermeability (Fig. 6*B*) but did not alter Ppa (area under the curve: control, 17.28 ± 4.3 cm H_2O × min; 1 µg of PLY, 15.30 ± 6.1 cm H_2O × min; n = 6). Hyperpermeability due both to PLY infu-

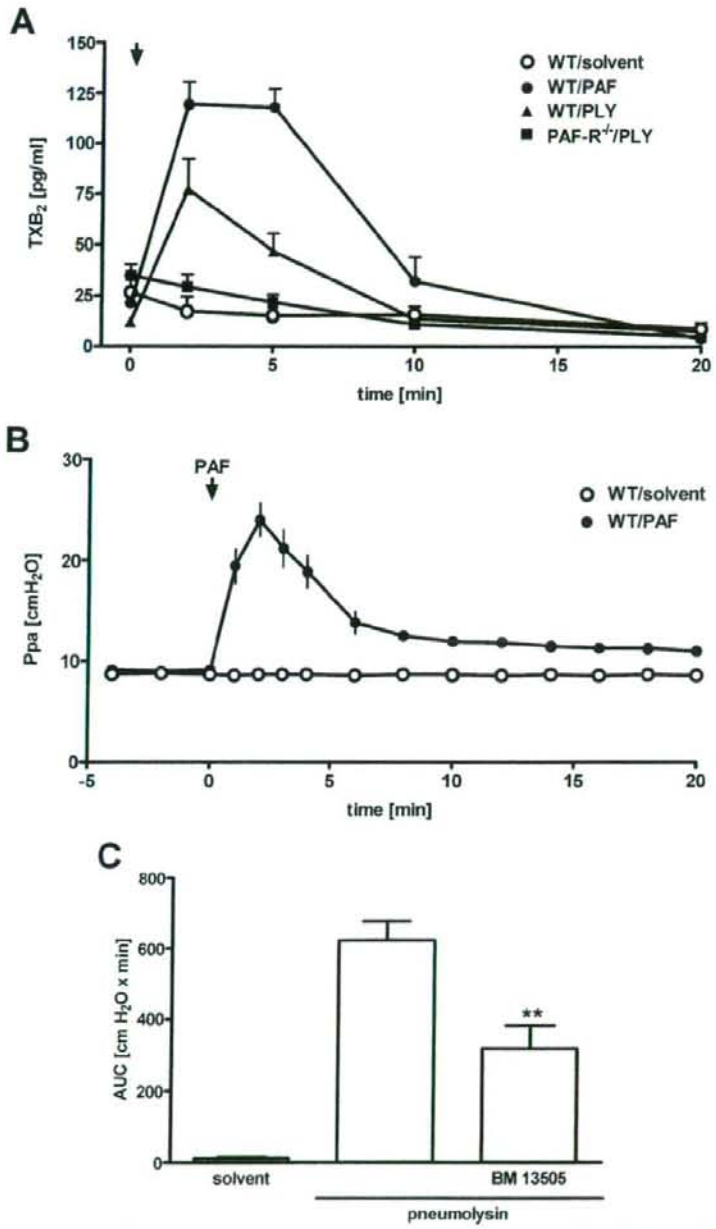

Figure 4. Pulmonary hypertension evoked by pneumolysin or platelet-activating factor (*PAF*) is partly mediated by thromboxane (TXA_2). *A*, TXB_2, a stable degradation product of TXA_2, was quantified in perfusion buffer sampled before and at 2, 5, 10, or 20 mins after pneumolysin (*PLY*) infusion (1 μg/min) in wild-type (*WT*) or PAF receptor–deficient ($PAF\text{-}R^{-/-}$) mice, or after PAF infusion (100 nM) in WT mice, respectively. PLY or PAF were infused for 1 min. *B*, pressure increases after PLY (1 μg/min) or PAF (100 nM) perfusion for 1 min are shown. *C*, the area under the pulmonary arterial pressure (*Ppa*) curve (*AUC*) values were reduced in PLY-challenged WT lungs preperfused with TXA_2 receptor antagonist BM 13505 (10 μM) compared with PLY-challenged WT lungs without BM 13505. $^{**}p < .01$ vs. WT/PLY.

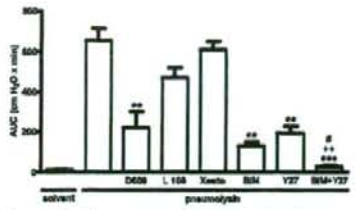

Figure 5. The pneumolysin-evoked pulmonary arterial pressure increase, as expressed by the area under the curve (*AUC*), was reduced in lungs preperfused with the phosphatidylcholine-specific phospholipase C inhibitor D 609 (100 μM) or with the protein kinase C inhibitor bisindolylmaleimide (*BIM*) (10 μM). The specific Rho-kinase inhibitor Y-27632 (*Y27*; 5 μM) also diminished the pulmonary arterial pressure increase, and the combination of BIM and Y-27632 showed additive effects. Inhibition of phosphatidylinositol-specific phospholipase C with L 108 (30 μM) or employment of the inositol trisphosphate receptor antagonist xestospongin C (*Xesto*; 10 μM) had no significant effect on pneumolysin-induced pulmonary hypertension. $^{**}p < .01$ vs. PLY; $^{***}p < .001$ vs. PLY; $^{\#}p < .05$ vs. PLY/BIM; $^{++}p < .01$ vs. PLY/Y27.

sion and to aerosolized PLY was decreased in lungs of $PAF\text{-}R^{-/-}$ mice.

DISCUSSION

The current study provides evidence that PLY-induced pulmonary hypertension and microvascular leakage is mediated by PAF. Isolated mouse lungs perfused with PLY responded with a rapid, dose-dependent increase of pulmonary vascular resistance, and increased amounts of PAF were measured in the tissue. Lungs of $PAF\text{-}R^{-/-}$ mice, and lungs of WT mice pretreated with a specific PAF-R antagonist, showed markedly reduced pressor responses. Both PLY- and exogenous PAF-induced hemodynamic alterations were accompanied by increased TXA_2 generation, and antagonism of the TXA_2 receptor diminished PLY-induced hypertension. Examination of downstream intracellular signaling pathways suggested major contributions of phosphatidylcholine-specific PLC and PKC and of the Rho-kinase pathway in PLY-induced pulmonary hypertension.

Several species of bacteria within the genera *Streptococcus*, *Clostridium*, *Bacillus*, and *Listeria* secrete cytolytic proteins that belong to the single, highly homologous family of thiol-activated, cholesterol-binding cytolysins. For lysation of cytoplasmic membranes, they require membrane cholesterol but no spe-

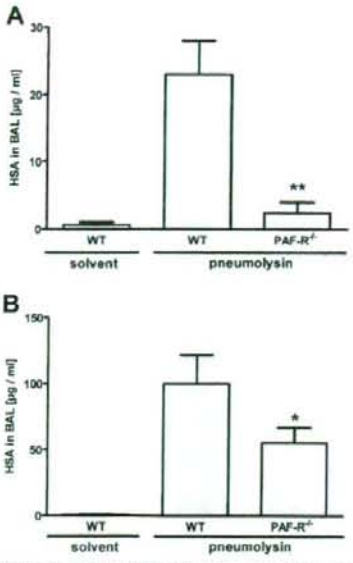

Figure 6. Pneumolysin-induced permeability was reduced in lungs of platelet-activating factor receptor deficient mice (*PAF-R*$^{-/-}$). Lungs were perfused with 0.04% human serum albumin (*HSA*). *A*, 1.0 μg/mL pneumolysin was infused for 1 min; *B*, 1.0 μg pneumolysin was aerosolized intratracheally. After 30 mins, bronchoalveolar lavage (*BAL*) was performed, and HSA was measured in BAL fluid. Pneumolysin evoked vascular leakage, as indicated by increased HSA concentration. *WT*, wild-type mice. $^{**}p < .01$ vs. WT/PLY; $^{*}p < .05$ vs. WT/PLY.

cific receptor (19). As a member of this family, PLY is an important virulence factor in pneumococcal disease, including pneumonia and sepsis (3, 4, 20–22), which is produced by all clinical isolates of *S. pneumoniae*. PLY-induced pore formation and cell lysation may be regarded as nonspecific, as compared with other members of this toxin family, but proinflammatory activities of PLY are important for the pathology of lung disease as well (23, 24). Correspondingly, PLY was a significant contributor to mortality in murine pneumococcal bacteremia (5) and sepsis (6). Purified PLY was capable of inducing major features of acute respiratory distress syndrome, including microvascular leakage and pulmonary hypertension, as we recently reported (7). In that study, endothelial localization of the toxin was noted in pulmonary arteries and in alveolar septs, and pulmonary arteries showing PLY immunostaining were exceedingly constricted. In contrast to WT PLY, Pd-B, a modified PLY with a single amino acid substitution at residue number 433 in the protein sequence (14), had no effect on Ppa in the present study, suggesting that the conserved undecapeptide sequence of PLY was responsible for vasoconstriction.

Addressing the mechanisms underlying the impressive PLY-induced lung damage, we employed ventilated, buffer-perfused mouse lungs. The model allows for measurement of fluid balance and real-time monitoring of lung hemodynamics on an intact organ level, independently from systemic inflammatory responses. In the current study, we did not focus on a potential role of blood components or recirculation phenomena.

The pulmonary PLY concentration in human pneumococcal pneumonia is not known. However, the PLY concentrations used in our study are in all probability realistic. Spreer et al. (25) observed that PLY levels in the cerebrospinal fluid during meningitis may reach 0.2 μg/mL, which is in the concentration range employed in our experiments. Moreover, in an intact mice model, we detected approximately 1×10^8 colony-forming units of *S. pneumoniae* in the lungs 6 hrs after infection, in parallel with significant lung injury (7). We do not exactly know the amount of PLY released from the pneumococci (NCTC 7978) in these *in vivo* experiments. However, *in vitro*, 1×10^8 of pneumococci of the same strain displayed a total hemolytic activity comparable with the hemolytic activity of 1.25 μg of recombinant PLY. Approximately 10% to 20% of the pneumococcal hemolytic activity were detected in the supernatant of bacterial cultures, which corresponds to the concentration range of recombinant PLY employed in our experiments. Thus, the PLY doses administered to the isolated perfused mice lungs may favorably compare with the PLY concentration in lungs of intact mice after infection with *S. pneumoniae*.

In endotoxin-induced acute lung inflammation, resident alveolar macrophages have been demonstrated to contribute to acute lung injury (26). Interestingly, early onset lung damage in intact mice challenged with PLY via the airways was independent of resident alveolar macrophages and newly recruited neutrophils and monocytes, suggesting direct pneumotoxicity of PLY (27). In line with these findings, we have recently demonstrated in a mouse model of pneumococcal pneumonia considerable lung microvascular leakage, which had already emerged at 6 hrs after transnasal infection. Significant neutrophil lung infiltration was not present at that point of time (7), suggesting that PLY substantially contributes to these early alterations. Therefore, the absence of circulating polymorphonuclear neutrophils and monocytes in our buffer-perfused lung model obviously does not play a major role for the rapid induction of severe lung damage by PLY.

Pneumococci firmly adhere to endothelial cells (28), and PLY released by these adherent pneumococci may thus directly affect the endothelium. Pulmonary endothelial cells synthesize and store several vasoactive mediators, including the proinflammatory phospholipid PAF (10, 29). Exotoxins of other pathogens, including *Escherichia coli* hemolysin and *Staphylococcus aureus* alpha-toxin, have been reported from our group to enhance PAF synthesis in endothelial cells (30, 31), and high PAF levels were detected in rat lungs after injection of lipopolysaccharide, mediating hemodynamic changes (32). Exogenous PAF potently contracted pulmonary vascular smooth muscle, causing pulmonary hypertension in rabbit and rat lungs (33, 34). Interestingly, PAF-R$^{-/-}$ mice had markedly reduced mortality in pneumococcal pneumonia (35) due to improved antibacterial host defense; however, pulmonary hemodynamics and lung injury were not examined in detail (35). We observed that perfusion of lungs with PLY resulted in increased PAF contents in the whole organ tissue. PAF synthesized by stimulated endothelial cells is not released into solution but almost completely remains cell associated (36), which may explain why PAF was not detectable in venous buffer effluate, despite increased tissue synthesis. Further evidence for an important role of PAF in PLY-induced pulmonary hypertension was provided by experiments employing lungs of PAF-R$^{-/-}$ mice, as these showed markedly reduced pressor responses compared with lungs of WT mice. In line with these findings, perfusion of lungs with the specific PAF-R antagonist BN 50730 before PLY infusion significantly decreased these pressor responses.

In isolated rabbit lungs, a thromboxane receptor antagonist diminished the pulmonary pressor response to PAF (34), and in rat lungs, PAF-induced smooth muscle contraction was largely mediated by thromboxane (TXA_2) and, to a smaller degree, by leukotrienes (37). In our model, intravascular PLY and exogenous PAF increased both Ppa and the content

of TXB_2, a stable degradation product of TXA_2, in the venous buffer effluate. Moreover, preperfusion with the thromboxane receptor antagonist BM 13505 distinctly reduced the PLY-induced pressor response in isolated mouse lungs. Some reduction was observed after lipoxygenase inhibition with AA-861 as well.

TXA_2 binds to the Gq-coupled thromboxane receptor. Gq-coupled receptors may activate 1) phosphatidylinositol-specific PLC (38), thereby increasing cytosolic IP_3 (38), and 2) phosphatidylcholine-specific PLC, resulting in diacylglycerol production. IP_3 induces cytosolic Ca^{2+} increase, followed by myosin light chain phosphorylation and subsequent smooth muscle contraction (38). Diacylglycerol activates PKC, leading to increased myosin light chain phosphorylation via diverse mechanisms (38). By using specific inhibitors, we demonstrated that the Ppa response to PLY in murine lungs depended primarily on phosphatidylcholine-specific PLC, but not phosphatidylinositol-specific PLC. Moreover, PLY-induced pressor responses were diminished after PKC inhibition but not altered by the potent IP_3-receptor antagonist xestospongin C. Consistent with these observations, xestospongin C failed to affect initial vasoconstriction to the thromboxane receptor agonist U46619 in perfused rat lungs (33). The concentration of xestospongin C employed in our experiments was three-fold above the median inhibitory concentration (39). Notably, at this concentration, xestospongin C prevented acetylcholine-induced calcium signaling in mouse lung slices (40) and attenuated PAF-induced edema formation in isolated rat lungs (41). Beyond IP_3 and PKC, activated Rho-kinase indirectly increases myosin light chain phosphorylation, thereby contributing to additional contractile force of myofilaments at fixed Ca^{2+} concentrations (42). Pretreatment with the Rho-kinase inhibitor Y-27632 (42) reduced the pressor response to PLY significantly. Although Y-27632 has been reported to alter TXA_2 generation in a recent study (33), the same work demonstrated extensive reduction of U46619-induced vasoconstriction by Rho-kinase inhibition in rat lungs (33), underscoring the importance of Rho-kinase in intracellular signal transduction subsequent to thromboxane receptor activation. In line with our results, this study further suggested a major role for Rho-kinase and found no contribution of the phosphatidylinositol-specific PLC and IP_3-dependent pathway in PAF- and TXA_2-induced pulmonary vasoconstriction (33).

The mechanism responsible for the residual pressor responses in PAF-$R^{-/-}$ mice remains speculative. Of note, combined PKC and Rho-kinase inhibition almost completely abolished the PLY-induced Ppa increases, underscoring the contribution of either pathway to PLY-induced pulmonary hypertension. Interestingly, a recent study demonstrated that sublytic concentrations of PLY produced rapid activation of Rho and Rac guanosine triphosphatases in neuroblastoma cells (43). However, a role of thromboxane-independent Rho-kinase activation by PLY in the lung has still to be defined.

In addition to pulmonary hypertension, microvascular leakage is an important feature of acute lung injury. We observed distinctly reduced permeability in lungs of PAF-$R^{-/-}$ mice stimulated with intravascular or aerosolized PLY. Notably, this reduction was not solely attributable to the decreased pressor response, as *aerosolized* PLY increased permeability without altering hemodynamics. As recently demonstrated, PAF-induced alterations in pulmonary vascular permeability are mediated by simultaneous activation of cyclooxygenase and acid sphingomyelinase, followed by subsequent production of prostaglandin E_2 and ceramide (44, 45). The contribution of these mechanisms to PLY-induced hyperpermeability requires further studies.

The implication of PAF in pulmonary disease has been clearly demonstrated in a variety of animal models, as recently reviewed (8). In humans, increased PAF levels have been found in pneumonia (46), acute respiratory distress syndrome (47), and sepsis (48, 49). However, there is only limited information on signaling pathways responsible for the responses to PAF in human tissue: PAF inhalation stimulated leukotriene and TXA_2 production in humans (50), and PAF activated PKC in human umbilical cord vein endothelial cells (51) and human epidermoid carcinoma cells (52) and activated Rho family proteins in human monocytic leukemia cells (53). These studies denote that a potential involvement of PAF in human pneumococcal pneumonia may include similar mechanisms as shown in our murine study.

In summary, our findings demonstrate a key role for PAF in PLY-induced pulmonary hypertension and microvascular leakage in mice, which are both hallmarks of acute lung injury. The PAF-R and its downstream signaling pathways may thus provide perspectives for specific pharmacologic interventions in pneumococci-evoked acute respiratory failure.

ACKNOWLEDGMENTS

We thank C. Thureau for BN 50730, A. C. Hocke for thoughtful discussions, and S. Preising, J. Thiele, and J. Ott for their skillful technical assistance.

REFERENCES

1. Ware LB, Matthay MA: The acute respiratory distress syndrome. *N Engl J Med* 2000; 342: 1334–1349
2. File TM: Community-acquired pneumonia. *Lancet* 2003; 362:1991–2001
3. Jedrzejas MJ: Pneumococcal virulence factors: Structure and function. *Microbiol Mol Biol Rev* 2001; 65:187–207
4. Mitchell TJ: Virulence factors and the pathogenesis of disease caused by *Streptococcus pneumoniae*. *Res Microbiol* 2000; 151: 413–419
5. Musher DM, Phan HM, Baughn RE: Protection against bacteremic pneumococcal infection by antibody to pneumolysin. *J Infect Dis* 2001; 183:827–830
6. Benton KA, Everson MP, Briles DE: A pneumolysin-negative mutant of *Streptococcus pneumoniae* causes chronic bacteremia rather than acute sepsis in mice. *Infect Immun* 1995; 63:448–455
7. Witzenrath M, Gutbier B, Hocke AC, et al: Role of pneumolysin for the development of acute lung injury in pneumococcal pneumonia. *Crit Care Med* 2006; 34:1947–1954
8. Uhlig S, Goggel R, Engel S: Mechanisms of platelet-activating factor (PAF)-mediated responses in the lung. *Pharmacol Rep* 2005; 57(Suppl):206–221
9. Wang H, Tan X, Chang H, et al: Regulation of platelet-activating factor receptor gene expression in vivo by endotoxin, platelet-activating factor and endogenous tumour necrosis factor. *Biochem J* 1997; 322:603–608
10. Prescott SM, Zimmerman GA, Stafforini DM, et al: Platelet-activating factor and related lipid mediators. *Annu Rev Biochem* 2000; 69:419–445
11. Ishii S, Kuwaki T, Nagase T, et al: Impaired anaphylactic responses with intact sensitivity to endotoxin in mice lacking a platelet-activating factor receptor. *J Exp Med* 1998; 187:1779–1788
12. von Bethmann AN, Brasch F, Nusing R, et al: Hyperventilation induces release of cytokines from perfused mouse lung. *Am J Respir Crit Care Med* 1998; 157:263–272
13. Paton JC, Andrew PW, Boulnois GJ, et al: Molecular analysis of the pathogenicity of *Streptococcus pneumoniae*: The role of pneumococcal proteins. *Annu Rev Microbiol* 1993; 47:89–115

14. Paton JC, Lock RA, Lee CJ, et al: Purification and immunogenicity of genetically obtained pneumolysin toxoids and their conjugation to *Streptococcus pneumoniae* type 19F polysaccharide. *Infect Immun* 1991; 59: 2297–2304
15. Seybold J, Thomas D, Witzenrath M, et al: Tumor necrosis factor-alpha-dependent expression of phosphodiesterase 2: Role in endothelial hyperpermeability. *Blood* 2005; 105:3569–3576
16. Owen JS, Wykle RL, Samuel MP, et al: An improved assay for platelet-activating factor using HPLC-tandem mass spectrometry. *J Lipid Res* 2005; 46:373–382
17. Lowry OH, Rosebrough NJ, Farr AL, et al: Protein measurement with the Folin phenol reagent. *J Biol Chem* 1951; 193:265–275
18. Clay KL: Quantitation of platelet-activating factor by gas chromatography-mass spectrometry. *Methods Enzymol* 1990; 187: 134–142
19. Palmer M: The family of thiol-activated, cholesterol-binding cytolysins. *Toxicon* 2001; 39:1681–1689
20. Cockeran R, Anderson R, Feldman C: The role of pneumolysin in the pathogenesis of *Streptococcus pneumoniae* infection. *Curr Opin Infect Dis* 2002; 15:235–239
21. Hirst RA, Kadioglu A, O'Callaghan C, et al: The role of pneumolysin in pneumococcal pneumonia and meningitis. *Clin Exp Immunol* 2004; 138:195–201
22. Paton JC: The contribution of pneumolysin to the pathogenicity of *Streptococcus pneumoniae*. *Trends Microbiol* 1996; 4:103–106
23. Rubins JB, Charboneau D, Fasching C, et al: Distinct roles for pneumolysin's cytotoxic and complement activities in the pathogenesis of pneumococcal pneumonia. *Am J Respir Crit Care Med* 1996; 153:1339–1346
24. Jounblat R, Kadioglu A, Mitchell TJ, et al: Pneumococcal behavior and host responses during bronchopneumonia are affected differently by the cytolytic and complement-activating activities of pneumolysin. *Infect Immun* 2003; 71:1813–1819
25. Spreer A, Lis A, Gerber J, et al: Differences in clinical manifestation of *Streptococcus pneumoniae* infection are not correlated with in vitro production and release of the virulence factors pneumolysin and lipoteichoic and teichoic acids. *J Clin Microbiol* 2004; 42:3342–3345
26. Maus UA, Koay MA, Delbeck T, et al: Role of resident alveolar macrophages in leukocyte traffic into the alveolar air space of intact mice. *Am J Physiol Lung Cell Mol Physiol* 2002; 282:L1245–L1252
27. Maus UA, Srivastava M, Paton JC, et al: Pneumolysin-induced lung injury is independent of leukocyte trafficking into the alveolar space. *J Immunol* 2004; 173:1307–1312
28. Cundell DR, Gerard NP, Gerard C, et al: *Streptococcus pneumoniae* anchor to activated human cells by the receptor for platelet-activating factor. *Nature* 1995; 377:435–438
29. Prescott SM, Zimmerman GA, McIntyre TM: Human endothelial cells in culture produce platelet-activating factor (1-alkyl-2-acetyl-sn-glycero-3-phosphocholine) when stimulated with thrombin. *Proc Nat Acad Sci U S A* 1984; 81:3534–3538
30. Krull M, Dold C, Hippenstiel S, et al: *Escherichia coli* hemolysin and *Staphylococcus aureus* alpha-toxin potently induce neutrophil adhesion to cultured human endothelial cells. *J Immunol* 1996; 157:4133–4140
31. Suttorp N, Buerke M, Tannert-Otto S: Stimulation of PAF-synthesis in pulmonary artery endothelial cells by *Staphylococcus aureus* alpha-toxin. *Thromb Res* 1992; 67:243–252
32. Chang SW, Feddersen CO, Henson PM, et al: Platelet-activating factor mediates hemodynamic changes and lung injury in endotoxin-treated rats. *J Clin Invest* 1987; 79:1498–1509
33. Martin C, Goggel R, Ressmeyer AR, et al: Pressor responses to platelet-activating factor and thromboxane are mediated by Rho-kinase. *Am J Physiol Lung Cell Mol Physiol* 2004; 287:L250–L257
34. Salzer WL, McCall CE: Primed stimulation of isolated perfused rabbit lung by endotoxin and platelet activating factor induces enhanced production of thromboxane and lung injury. *J Clin Invest* 1990; 85:1135–1143
35. Rijneveld AW, Weijer S, Florquin S, et al: Improved host defense against pneumococcal pneumonia in platelet-activating factor receptor-deficient mice. *J Infect Dis* 2004; 189:711–716
36. McIntyre TM, Zimmerman GA, Prescott SM: Leukotrienes C4 and D4 stimulate human endothelial cells to synthesize platelet-activating factor and bind neutrophils. *Proc Nat Acad Sci U S A* 1986; 83:2204–2208
37. Uhlig S, Wollin L, Wendel A: Contributions of thromboxane and leukotrienes to PAF-induced impairment of lung function in the rat. *J Appl Physiol* 1994; 77:262–269
38. Harnett KM, Biancani P: Calcium-dependent and calcium-independent contractions in smooth muscles. *Am J Med* 2003; 115(Suppl 3A):24S–30S
39. Gafni J, Munsch JA, Lam TH, et al: Xestospongins: Potent membrane permeable blockers of the inositol 1,4,5-trisphosphate receptor. *Neuron* 1997; 19:723–733
40. Bergner A, Sanderson MJ: ATP stimulates Ca^{2+} oscillations and contraction in airway smooth muscle cells of mouse lung slices. *Am J Physiol Lung Cell Mol Physiol* 2002; 283:L1271–L1279
41. Göggel R, Uhlig S: PAF-induced edema is mediated partly by activation of the inositol trisphosphate (IP_3)-receptor. Abstr. *Am J Respir Crit Care Med* 2000; 161:A418
42. Uehata M, Ishizaki T, Satoh H, et al: Calcium sensitization of smooth muscle mediated by a Rho-associated protein kinase in hypertension. *Nature* 1997; 389:990–994
43. Iliev AI, Djannatian JR, Nau R, et al: Cholesterol-dependent actin remodeling via RhoA and Rac1 activation by the *Streptococcus pneumoniae* toxin pneumolysin. *Proc Nat Acad Sci U S A* 2007; 104:2897–2902
44. Göggel R, Hoffman S, Nusing R, et al: Platelet-activating factor-induced pulmonary edema is partly mediated by prostaglandin E(2), E-prostanoid 3-receptors, and potassium channels. *Am J Respir Crit Care Med* 2002; 166:657–662
45. Göggel R, Winoto-Morbach S, Vielhaber G, et al: PAF-mediated pulmonary edema: A new role for acid sphingomyelinase and ceramide. *Nat Med* 2004; 10:155–160
46. Nakos G, Tsangaris H, Liokatis S, et al: Ventilator-associated pneumonia and atelectasis: Evaluation through bronchoalveolar lavage fluid analysis. *Intensive Care Med* 2003; 29: 555–563
47. Nakos G, Kitsiouli EI, Tsangaris I, et al: Bronchoalveolar lavage fluid characteristics of early intermediate and late phases of ARDS: Alterations in leukocytes, proteins, PAF and surfactant components. *Intensive Care Med* 1998; 24:296–303
48. Bussolino F, Porcellini MG, Varese L, et al: Intravascular release of platelet activating factor in children with sepsis. *Thromb Res* 1987; 48:619–620
49. Sorensen J, Kald B, Tagesson C, et al: Platelet-activating factor and phospholipase A2 in patients with septic shock and trauma. *Intensive Care Med* 1994; 20:555–561
50. Taylor IK, Ward PS, Taylor GW, et al: Inhaled PAF stimulates leukotriene and thromboxane A2 production in humans. *J Appl Physiol* 1991; 71:1396–1402
51. Bussolino F, Silvagno F, Garbarino G, et al: Human endothelial cells are targets for platelet-activating factor (PAF): Activation of alpha and beta protein kinase C isozymes in endothelial cells stimulated by PAF. *J Biol Chem* 1994; 269:2877–2886
52. Tripathi YB, Lim RW, Fernandez-Gallardo S, et al: Involvement of tyrosine kinase and protein kinase C in platelet-activating-factor-induced c-fos gene expression in A-431 cells. *Biochem J* 1992; 286:527–533
53. Sumita C, Yamane M, Matsuda T, et al: Platelet activating factor induces cytoskeletal reorganization through Rho family pathway in THP-1 macrophages. *FEBS Lett* 2005; 579: 4038–4042

balt2/zjh-jpath/zjh-jpath/zjh00308/zjh7551-08z | xppws | S=1 | 1/21/08 | 4:55 | 4/Color Figure(s): F1–4,F6–7 | Art: AJP07-0834 | Input-krb

The American Journal of Pathology, Vol. 172, No. 3, March 2008

DOI: 10.2353/ajpath.2008.070834

Endothelial Cysteinyl Leukotriene 2 Receptor Expression Mediates Myocardial Ischemia-Reperfusion Injury

AQ:A-B

Wei Jiang,* Sean R. Hall,* Michael P.W. Moos,* Richard Yang Cao,* Satoshi Ishii,† Kofo O. Ogunyankin,‡ Luis G. Melo,*‡ and Colin D. Funk*§

From the Departments of Physiology, Medicine,† and Biochemistry,§ Queen's University, Kingston, Canada; and the Department of Biochemistry and Molecular Biology,‡ University of Tokyo, Tokyo, Japan*

Cysteinyl leukotrienes (CysLTs) have been implicated as inflammatory mediators of cardiovascular disease. Three distinct CysLT receptor subtypes transduce the actions of CysLTs but the role of the endothelial CysLT$_2$ receptor (CysLT$_2$R) in cardiac function is unknown. Here, we investigated the role of CysLT$_2$R in myocardial ischemia-reperfusion (I/R) injury using transgenic (tg) mice overexpressing human CysLT$_2$R in vascular endothelium and nontransgenic (ntg) littermates. Infarction size in tg mice increased 114% compared with ntg mice 48 hours after I/R; this increase was blocked by the CysLT receptor antagonist BAY-u9773. Injection of ^{125}I-albumin into the systemic circulation revealed significantly enhanced extravasation of the label in tg mice, indicating increased leakage of the coronary endothelium, combined with increased incidence of hemorrhage and cardiomyocyte apoptosis. Expression of proinflammatory genes such as Egr-1, VCAM-1, and ICAM was significantly increased in tg mice relative to ntg controls. Echocardiographic assessment 2 weeks after I/R revealed decreased anterior wall thickness in tg mice. Furthermore, the postreperfusion time constant τ of isovolumic relaxation was significantly increased in tg animals, indicating diastolic dysfunction. These results reveal that endothelium-targeted overexpression of CysLT$_2$R aggravates myocardial I/R injury by increasing endothelial permeability and exacerbating inflammatory gene expression, leading to accelerated left ventricular remodeling, induction of peri-infarct zone cellular apoptosis, and impaired cardiac performance. ***(Am J Pathol 2008, 172:000–000; DOI: 10.2353/ajpath.2008.070834)***

Myocardial infarction results from severe impairment of the coronary blood supply usually provoked by thrombotic or other acute alterations of coronary atherosclerotic plaque.[1] It remains the chief cause of death in North America and Europe.[2] With loss of oxygen supply, apoptosis and necrosis of cardiac myocytes in the ischemic area ensues leading to decreased cardiac performance.[3] Rapid reperfusion is essential to limit the extent of myocardial necrosis. However, the consequences of reperfusion are complex and include various deleterious effects collectively referred to as ischemia-reperfusion (I/R) injury.[3] The intense inflammatory response after reperfusion plays a central role not only in promoting tissue injury, but also in repair after infarction.[4] The inflammatory process characterizing early and late reperfusion is an important aspect of the changes leading to tissue damage.[4] Increased vascular permeability and expression of adhesion molecules initiates the inflammatory reaction, and alterations of endothelial function are pivotal in the development of reperfusion damage.[4,5] Fn1

Cysteinyl leukotrienes (CysLTs), leukotriene C_4 (LTC_4), leukotriene D_4 (LTD_4), and leukotriene E_4 (LTE_4), are well established inflammatory agents that mediate bronchial and vascular smooth muscle constriction and enhance vascular permeability.[6] CysLTs are implicated in inflammatory conditions such as asthma and more recently in cardiovascular disease.[7–9] CysLTs mediate their actions via G protein-coupled receptor (GPCR) proteins, cysteinyl leukotriene 1 receptor (CysLT$_1$R), cysteinyl leukotriene 2 receptor (CysLT$_2$R), and a recently deorphanized GPCR known as GPR17.[6,10] The CysLT$_2$R gene is ex-

Supported by the Canadian Institutes of Health Research (grants MOP 68930 to C.D.F. and MOP 79506 to L.G.M.), the Heart and Stroke Foundation of Ontario (grant NA 5779 to L.G.M.), and the Pharmacological Society of Canada (Merck Frosst postdoctoral fellowship to S.R.H.).

Accepted for publication November 20, 2007.

This publication is dedicated to the honor of Luis G. Melo who passed away suddenly after a brief and courageous battle with pancreatic cancer.

C.D.F. and L.G.M. hold Canada Research Chairs. C.D.F. is a career investigator of the Heart and Stroke Foundation of Ontario.

Address reprint requests to Colin D. Funk, Department of Physiology, 433 Botterell Hall, Stuart St., Queen's University, Kingston, ON K7L 3N6 Canada. E-mail: funkc@queensu.ca.

balt2/zjh-jpath/zjh-jpath/zjh00308/zjh7551-08z | xppws | S=1 | 1/21/08 | 4:55 | 4/Color Figure(s): F1-4,F6-7 | Art: AJP07-0834 | Input-krb

pressed in human heart and coronary vessels, also within the cardiac Purkinje system, as well as in human coronary smooth muscle cells and umbilical vein endothelial cells.[8,11-14] $CysLT_2R$ expression in mouse heart appears to be more restricted with diffuse expression within endothelial cells.[15] We generated previously transgenic (tg) mice overexpressing the human $CysLT_2R$ in vascular endothelium to characterize the role of this receptor in vascular function.[16]

The involvement of CysLTs and their receptors in inflammation and fibrosis has been confirmed in various animal and human studies.[17] Several studies reported enhanced edema and neutrophil infiltration after myocardial I/R concomitant with elevation of CysLTs.[18,19] These eicosanoids are detected as increased urinary LTE_4 levels in patients after admission for suspected acute myocardial infarction and unstable angina.[20] Moreover, the expression of $CysLT_1R$ and $CysLT_2R$ is increased in organs that are prone to ischemic damage and $CysLT_1R$ antagonism exerts anti-inflammatory effects on cerebral and renal I/R injury.[21-23] Few studies have investigated CysLTs and their receptors in acute myocardial infarction and specifically the role of $CysLT_2R$ in myocardial I/R injury has not been established. Here, we report that endothelium-targeted overexpression of $CysLT_2R$ aggravates myocardial I/R injury by increasing endothelial permeability and exacerbating inflammatory gene expression, leading to accelerated left ventricular (LV) remodeling and impaired cardiac performance.

Materials and Methods

Animals

The generation of EC-$CysLT_2R$ transgenic mice has been described previously.[16] These mice express seven copies of the human $CysLT_2R$ gene under control of the Tie2 promoter/enhancer, integrated in a gene-sparse region of chromosome 6. Hemizygous mice were continuously backcrossed with C57BL/6 mice to obtain equal numbers of transgenic and wild-type littermates. 5-Lipoxygenase-deficient ($5LO^{-/-}$) mice, developed in our laboratory previously,[24] were obtained from The Jackson Laboratory (Bar Harbor, ME). The mice were backcrossed for more than nine generations to the C57BL/6 background. The $5LO^{-/-}$ mice show absence of 5-lipoxygenase mRNA, protein, and leukotriene synthesis in inflammatory cells. $CysLT_2R$-deficient LacZ mice were generated by standard gene targeting procedures using C57BL/6 embryonic stem cells (S. Ishii, unpublished data) and embryos heterozygous for the genetic modification were transferred from Japan, revived at Queen's University, and littermates of heterozygous offspring (all on a C57BL/6 genetic background) were used in these studies.

Mouse Model of Myocardial I/R and Drug Treatment

Mice (8 to 12 weeks) underwent coronary artery occlusion or sham surgery as previously described.[25] Briefly, mice were anesthetized with sodium pentobarbital (45 mg/kg) intraperitoneally, intubated, and ventilated with a rodent ventilator (Harvard Apparatus, St. Laurent, Canada). A midsternal thoracotomy was performed at the fourth intercostal space to expose the anterior surface of the heart. The proximal left anterior descending artery (LAD) was identified and a 6-0 silk Ethilon suture was placed around the artery and surrounding myocardium just below the atrioventricular border. Regional ischemia was induced for 30 minutes by tightening the suture against a small piece of PE-10 tubing placed on top of the LAD. Ischemia was confirmed by the discoloration of the myocardium. Sham-operated animals served as surgical controls and were subjected to the same surgical procedures as the experimental animals, with the exception that the LAD was not ligated. At the end of ischemia, the ligature was loosened and reperfusion was achieved. The lungs were reinflated and the muscle and skin layers were closed separately. The animals were weaned from the ventilator, extubated, and allowed to recover under a heat lamp before being returned to their cages. For animals receiving drug treatment, Bay-u9773 (0.25 mg/kg; Biomol Research Products, Plymouth Meeting, PA) was diluted in 1% phosphate-buffered saline (PBS) and injected intraperitoneally 2 hours before surgery, and 2, 8, and 16 hours after reperfusion. Surgical procedures and treatment regimens were approved by the University Animal Care Committee at Queen's University and adhered to the guidelines of the Canadian Council of Animal Care and the Guiding Principles in the Care and Use of Animals of the American Physiological Society.

Morphometric Evaluation of Risk Area and Infarction Size

Forty-eight hours after reperfusion, mice were euthanized by an intraperitoneal pentobarbital overdose. The 48-hour time point was selected because it is commonly used to assess early inflammatory events (eg, leukocyte infiltration, vascular leakage). The heart was exposed and the original suture was religated. The heart was then perfused retrogradely with 100 to 200 μl of 2% Evans blue dye in PBS (pH 7.4) to delineate the nonischemic area. The heart was excised and rinsed in ice-cold PBS and the LV, including the interventricular septum, was sectioned into four or five slices of similar thickness perpendicular to the long axis of the heart. The slices were incubated in 1% 2,3,5-triphenyltetrazolium chloride (TTC; Sigma Chemicals, St. Louis, MO) at 37°C for 15 minutes to demarcate viable and necrotic tissue. The thickness of each slice was measured using calipers. The slices were photographed on both sides with a digital camera (Canon Corp., Tokyo, Japan). The infarct area (pale white), the area at risk (area excluding Evans Blue), and the total left ventricular area were traced and calculated for both sides of each slice using Image software (National Institutes of Health, Bethesda, MD). The areas for each slice were multiplied by the thickness of the slice to obtain a measure of volume. The cumulative volume for all sections for each heart was used for comparisons. The size